The Journal of Child Psychology and Psychiatry

Journal of Child Psychology and Psychiatry 62:10 (2021), pp 1202–1219 doi:10.1111/jcpp.13396

Analysis of structural brain asymmetries in attention-deficit/hyperactivity disorder in 39 datasets

Merel C. Postema,[1] Martine Hoogman,[2,3] Sara Ambrosino,[4] Philip Asherson,[5] Tobias Banaschewski,[6] Cibele E. Bandeira,[7,8] Alexandr Baranov,[9] Claiton H.D. Bau,[7,8,10] Sarah Baumeister,[6] Ramona Baur-Streubel,[11] Mark A. Bellgrove,[12] Joseph Biederman,[13,14] Janita Bralten,[2,3] Daniel Brandeis,[15,16] Silvia Brem,[16,17] Jan K. Buitelaar,[18,19] Geraldo F. Busatto,[20] Francisco X. Castellanos,[21,22] Mara Cercignani,[23] Tiffany M. Chaim-Avancini,[20] Kaylita C. Chantiluke,[24] Anastasia Christakou,[24,25] David Coghill,[26,27] Annette Conzelmann,[28,29] Ana I. Cubillo,[24] Renata B. Cupertino,[7,8] Patrick de Zeeuw,[30] Alysa E. Doyle,[14,31] Sarah Durston,[30] Eric A. Earl,[32] Jeffery N. Epstein,[33,34] Thomas Ethofer,[35] Damien A. Fair,[32] Andreas J. Fallgatter,[36,37] Stephen V. Faraone,[38] Thomas Frodl,[39,40] Matt C. Gabel,[23] Tinatin Gogberashvili,[41] Eugenio H. Grevet,[7,8,10] Jan Haavik,[42,43] Neil A. Harrison,[23,44] Catharina A. Hartman,[45] Dirk J. Heslenfeld,[46] Pieter J. Hoekstra,[47] Sarah Hohmann,[6] Marie F. Høvik,[43,48] Terry L. Jernigan,[49] Bernd Kardatzki,[50] Georgii Karkashadze,[9] Clare Kelly,[51,52] Gregor Kohls,[53] Kerstin Konrad,[53,54] Jonna Kuntsi,[5] Luisa Lazaro,[55,56] Sara Lera-Miguel,[57] Klaus-Peter Lesch,[58,59,60] Mario R. Louza,[61] Astri J. Lundervold,[42,62] Charles B Malpas,[63,64] Paulo Mattos,[65,66] Hazel McCarthy,[40,67] Leyla Namazova-Baranova,[9,68] Rosa Nicolau,[69] Joel T. Nigg,[32,70] Stephanie E. Novotny,[71] Eileen Oberwelland Weiss,[72,73] Ruth L. O'Gorman Tuura,[74,75] Jaap Oosterlaan,[76,77] Bob Oranje,[30] Yannis Paloyelis,[78] Paul Pauli,[79] Felipe A. Picon,[7] Kerstin J. Plessen,[80,81] J. Antoni Ramos-Quiroga,[82,83,84,85] Andreas Reif,[86] Liesbeth Reneman,[87] Pedro G.P. Rosa,[20] Katya Rubia,[24] Anouk Schrantee,[88] Lizanne J.S. Schweren,[45] Jochen Seitz,[89] Philip Shaw,[90] Tim J. Silk,[91,92] Norbert Skokauskas,[93,94] Juan C. Soliva Vila,[95] Michael C. Stevens,[71,96] Gustavo Sudre,[97] Leanne Tamm,[98,99] Fernanda Tovar-Moll,[65,100] Theo G.M. van Erp,[101,102] Alasdair Vance,[103] Oscar Vilarroya,[95,104] Yolanda Vives-Gilabert,[105] Georg G. von Polier,[89,106] Susanne Walitza,[17] Yuliya N. Yoncheva,[107] Marcus V. Zanetti,[108,109] Georg C. Ziegler,[58] David C. Glahn,[71,110] Neda Jahanshad,[111] Sarah E. Medland,[112] ENIGMA ADHD Working Group, Paul M. Thompson,[113] Simon E. Fisher,[1,3] Barbara Franke,[2,3,114] and Clyde Francks[1,3]

[1]Language and Genetics Department, Max Planck Institute for Psycholinguistics, Nijmegen, The Netherlands; [2]Department of Human Genetics, Radboud University Medical Center, Nijmegen, Netherlands; [3]Donders Institute for Brain, Cognition and Behaviour, Radboud University, Nijmegen, Netherlands; [4]NICHE lab, Department of Psychiatry, University Medical Center Utrecht Brain Center, Utrecht University, Utrecht, The Netherlands; [5]Social, Genetic and Developmental Psychiatry Centre, Institute of Psychiatry, Psychology and Neuroscience, King's College London, London, UK; [6]Department of Child and Adolescent Psychiatry and Psychotherapy, Central Institute of Mental Health, Medical Faculty Mannheim/Heidelberg University, Mannheim, Germany; [7]Adulthood ADHD Outpatient Program (ProDAH), Clinical Research Center, Hospital de Clínicas de Porto Alegre, Porto Alegre, Brazil; [8]Department of Genetics, Institute of Biosciences, Universidade Federal do Rio Grande do Sul, Porto Alegre, Brazil; [9]Research Institute of Pediatrics and Child Health of Central Clinical Hospital of the Russian Academy of Sciences of the Ministry of Science and Higher Education of the Russian Federation, Moscow, Russia; [10]Developmental Psychiatry Program, Experimental Research Center, Hospital de Clínicas de Porto Alegre, Porto Alegre, Brazil; [11]Department of Biological Psychology, Clinical Psychology and Psychotherapy, University of Würzburg, Würzburg, Germany; [12]Turner Institute for Brain and Mental Health and School of Psychological Sciences, Monash University, Melbourne, Vic., Australia; [13]Clinical and Research Programs in Pediatric Psychopharmacology and Adult ADHD, Boston, MA, USA; [14]Department of Psychiatry, Massachusetts General Hospital, Harvard Medical School, Boston, MA, USA; [15]Department of Child and Adolescent Psychiatry and Psychotherapy, Psychiatric Hospital, University of Zurich, Zurich, Switzerland; [16]The Neuroscience Center Zurich, University of Zurich and ETH Zurich, Zurich, Switzerland; [17]Department of Child and Adolescent Psychiatry and Psychotherapy, Psychiatric Hospital, University of Zurich, Zurich, Switzerland; [18]Department of Cognitive Neuroscience, Donders Institute for Brain, Cognition and Behaviour, Radboudumc, Nijmegen, The Netherlands; [19]Karakter Child and Adolescent Psychiatry University Center, Nijmegen, The Netherlands; [20]Laboratory of Psychiatric Neuroimaging (LIM-21, Department and Institute of Psychiatry, Hospital das Clinicas HCFMUSP, Faculty of Medicine, University of São Paulo, Sao Paulo, Sao Paulo, Brazil; [21]Department of Child and Adolescent Psychiatry, NYU Grossman School of Medicine, New York, NY, USA; [22]Nathan Kline Institute for Psychiatric Research, Orangeburg, NY, USA; [23]Department of Neuroscience, Brighton and Sussex Medical School, Falmer, Brighton, UK; [24]Department of Child and Adolescent Psychiatry, Institute of Psychiatry, Psychology and Neuroscience, King's College London, London, UK; [25]School of Psychology and Clinical Language Sciences, Centre for Integrative Neuroscience and Neurodynamics, University of Reading,

Reading, UK; [26]Departments of Paediatrics and Psychiatry, University of Melbourne, Melbourne, Vic., Australia; [27]Murdoch Children's Research Institute, Melbourne, Vic., Australia; [28]Department of Child and Adolescent Psychiatry, Psychosomatics and Psychotherapy, University Hospital of Tübingen, Tübingen, Germany; [29]Department of Psychology (Clinical Psychology II), PFH – Private University of Applied Sciences, Göttingen, Germany; [30]NICHE Lab, Department of Psychiatry, Brain Center Rudolf Magnus, University Medical Center Utrecht, Utrecht, The Netherlands; [31]Center for Genomic Medicine, Massachusetts General Hospital, Harvard Medical School, Boston, MA, USA; [32]Department of Behavioral Neuroscience, Oregon Health & Science University, Portland, OR, USA; [33]Division of Behavioral Medicine and Clinical Psychology, Cincinnati Children's Hospital Medical Center, Cincinnati, OH, USA; [34]Department of Pediatrics, University of Cincinnati College of Medicine, Cincinnati, OH, USA; [35]Clinic for Psychiatry/Psychotherapy Tübingen/Department for Biomedical Magnetic Resonance, Tübingen, Germany; [36]Department of Psychiatry and Psychotherapy, University Hospital of Tuebingen, Tuebingen, Germany; [37]LEAD Graduate School, University of Tuebingen, Tübingen, Germany; [38]Departments of Psychiatry and of Neuroscience and Physiology, SUNY Upstate Medical University, Syracuse, NY, USA; [39]Department of Psychiatry and Psychotherapy, Otto von Guericke University, Magdeburg, Germany; [40]Department of Psychiatry, Trinity College Dublin, Dublin, Ireland; [41]Laboratory of Neurology and Cognitive Health, National Medical Research Center for Children's Health, Moscow, Russia; [42]Department of Biomedicine, K.G. Jebsen Centre for Neuropsychiatric Disorders, University of Bergen, Bergen, Norway; [43]Division of Psychiatry, Haukeland University Hospital, Bergen, Norway; [44]Sussex Partnership NHS Foundation Trust, Swandean, East Sussex, UK; [45]Department of Psychiatry, Interdisciplinary Center Psychopathology and Emotion Regulation (ICPE), University Medical Center Groningen, University of Groningen, Groningen, The Netherlands; [46]Faculty of Behavioural and Movement Sciences, Vrije Universiteit Amsterdam, Amsterdam, The Netherlands; [47]Department of Child and Adolescent Psychiatry, University Medical Center Groningen, University of Groningen, Groningen, The Netherlands; [48]Department of Clinical Medicine, University of Bergen, Bergen, Norway; [49]Center for Human Development, UC San Diego, La Jolla, CA, USA; [50]Department of Biomedical Magnetic Resonance, University of Tuebingen, Tuebingen, Germany; [51]School of Psychology and Department of Psychiatry at the School of Medicine, Trinity College Dublin, Ireland; [52]Trinity College Institute of Neuroscience, Trinity College Dublin, Dublin, Ireland; [53]Child Neuropsychology Section, Department of Child and Adolescent Psychiatry, Psychosomatics, and Psychotherapy, University Hospital RWTH, Aachen, Germany; [54]JARA Institute Molecular Neuroscience and Neuroimaging (INM-11), Institute for Neuroscience and Medicine, Research Center Jülich, Jülich, Germany; [55]Institut d'Investigacions Biomèdiques August Pi i Sunyer (IDIBAPS), Biomedical Network Research Center on Mental Health (CIBERSAM), Barcelona, Spain; [56]Department of Medicine, University of Barcelona, Barcelona, Spain; [57]Department of Child and Adolescent Psychiatry and Psychology, Institute of Neurosciencies, Hospital Clinic, Barcelona, Spain; [58]Division of Molecular Psychiatry, Center of Mental Health, University of Würzburg, Würzburg, Germany; [59]Laboratory of Psychiatric Neurobiology, Institute of Molecular Medicine, I.M. Sechenov First Moscow State Medical University, Moscow, Russia; [60]Department of Psychiatry and Neuropsychology, School for Mental Health and Neuroscience (MHeNS), Maastricht University, Maastricht, The Netherlands; [61]Institute of Psychiatry, Faculty of Medicine, University of São Paulo, São Paulo, Brazil; [62]Department of Biological and Medical Psychology, University of Bergen, Bergen, Norway; [63]Developmental Imaging Group, Murdoch Children's Research Institute, Melbourne, Vic., Australia; [64]Clinical Outcomes Research Unit (CORe), Department of Medicine, Royal Melbourne Hospital, The University of Melbourne, Melbourne, Vic., Australia; [65]D'Or Institute for Research and Education, Rio de Janeiro, Brazil; [66]Federal University of Rio de Janeiro, Rio de Janeiro, Brazil; [67]Centre of Advanced Medical Imaging, St James's Hospital, Dublin, Ireland; [68]Russian National Research Medical University Ministry of Health of the Russian Federation, Moscow, Russia; [69]Department of Child and Adolescent Psychiatry and Psychology, Institut of Neurosciencies, Hospital Clinic, Barcelona, Spain; [70]Department of Psychiatry, Oregon Health & Science University, Portland, OR, USA; [71]Olin Neuropsychiatry Research Center, Hartford Hospital, Hartford, CT, USA; [72]Translational Neuroscience, Child and Adolescent Psychiatry, University Hospital RWTH Aachen, Aachen, Germany; [73]Cognitive Neuroscience (INM-3), Institute for Neuroscience and Medicine, Research Center Jülich, Jülich, Germany; [74]Center for MR Research, University Children's Hospital, Zurich, Switzerland; [75]Zurich Center for Integrative Human Physiology (ZIHP), Zurich, Switzerland; [76]Clinical Neuropsychology Section, Vrije Universiteit Amsterdam, Amsterdam, The Netherlands; [77]Emma Neuroscience Group, Department of Pediatrics, Amsterdam Reproduction & Development, Emma Children's Hospital Amsterdam University Medical Centers, University of Amsterdam, Amsterdam, The Netherlands; [78]Department of Neuroimaging, Institute of Psychiatry, Psychology and Neuroscience, King's College London, London, UK; [79]Department of Psychology (Biological Psychology, Clinical Psychology and Psychotherapy) and Center of Mental Health, University of Würzburg, Würzburg, Germany; [80]Child and Adolescent Mental Health Centre, Capital Region Copenhagen, Copenhagen, Denmark; [81]Division of Child and Adolescent Psychiatry, Department of Psychiatry, University Hospital Lausanne, Lausanne, Switzerland; [82]Department of Psychiatry, Hospital Universitari Vall d'Hebron, Barcelona, Catalonia, Spain; [83]Group of Psychiatry, Mental Health and Addictions, Vall d'Hebron Research Institute (VHIR), Barcelona, Catalonia, Spain; [84]Biomedical Network Research Centre on Mental Health (CIBERSAM), Barcelona, Catalonia, Spain; [85]Department of Psychiatry and Legal Medicine, Universitat Autònoma de Barcelona, Barcelona, Catalonia, Spain; [86]Department of Psychiatry, Psychosomatic Medicine and Psychotherapy, University Hospital Frankfurt, Frankfurt, Germany; [87]Academic Medical Center, Amsterdam University Medical Center, Amsterdam, The Netherlands; [88]Department of Radiology and Nuclear Medicine, Amsterdam University Medical Centers, Amsterdam, The Netherlands; [89]Child and Adolescent Psychiatry, University Hospital RWTH Aachen, Aachen, Germany; [90]National Human Genome Research Institute and National Institute of Mental health, Bethesda, MD, USA; [91]School of Psychology, Deakin University, Geelong, Vic., Australia; [92]Murdoch Children's Research Institute, Developmental Imaging, Melbourne, Vic., Australia; [93]Centre for Child and Adolescent Mental Health, NTNU, Trondheim, Norway; [94]Institute of Mental Health, Norwegian University of Science and Technology, Trondheim, Norway; [95]Department of Psychiatry and Forensic Medicine, Universitat Autonoma de Barcelona, Barcelona, Spain; [96]Department of Psychiatry, Yale University School

of Medicine, New Haven, CT, USA; [97]National Human Genome Research Institute, Bethesda, MD, USA; [98]Department of Pediatrics, Cincinnati Children's Hospital Medical Center, Cincinnati, OH, USA; [99]College of Medicine, University of Cincinnati, Cincinnati, OH, USA; [100]Morphological Sciences Program, Federal University of Rio de Janeiro, Rio de Janeiro, Brazil; [101]Clinical Translational Neuroscience Laboratory, Department of Psychiatry and Human Behavior, University of California Irvine, Irvine, CA, USA; [102]Center for the Neurobiology of Learning and Memory, University of California Irvine, Irvine, CA, USA; [103]Department of Paediatrics, University of Melbourne, Parkville, Vic., Australia; [104]Hospital del Mar Medical Research Institute (IMIM), Barcelona, Spain; [105]Instituto ITACA, Universitat Politècnica de València, València, Spain; [106]Brain and Behavior (INM-7), Institute for Neuroscience and Medicine, Research Center Jülich, Jülich, Germany; [107]Department of Child and Adolescent Psychiatry, NYU Child Study Center, Hassenfeld Children's Hospital at NYU Langone, New York, NY, USA; [108]Department of Psychiatry, Faculty of Medicine, University of São Paulo, São Paulo, Brazil; [109]Hospital Sírio-Libanês, São Paulo, Brazil; [110]Department of Psychiatry, Boston Children's Hospital and Harvard Medical School, Boston, MA, USA; [111]Imaging Genetics Center, Stevens Neuroimaging and Informatics Institute, Keck School of Medicine of USC, Los Angeles, CA, USA; [112]Psychiatric Genetics, QIMR Berghofer Medical Research Institute, Brisbane, Qld, Australia; [113]Imaging Genetics Center, Stevens Institute for Neuroimaging & Informatics, Keck School of Medicine, University of Southern California, Los Angeles, CA, USA; [114]Department of Psychiatry, Radboud University Medical Center, Nijmegen, The Netherlands

Objective: Some studies have suggested alterations of structural brain asymmetry in attention-deficit/hyperactivity disorder (ADHD), but findings have been contradictory and based on small samples. Here, we performed the largest ever analysis of brain left-right asymmetry in ADHD, using 39 datasets of the ENIGMA consortium. **Methods:** We analyzed asymmetry of subcortical and cerebral cortical structures in up to 1,933 people with ADHD and 1,829 unaffected controls. Asymmetry Indexes (AIs) were calculated per participant for each bilaterally paired measure, and linear mixed effects modeling was applied separately in children, adolescents, adults, and the total sample, to test exhaustively for potential associations of ADHD with structural brain asymmetries. **Results:** There was no evidence for altered caudate nucleus asymmetry in ADHD, in contrast to prior literature. In children, there was less rightward asymmetry of the total hemispheric surface area compared to controls ($t = 2.1$, $p = .04$). Lower rightward asymmetry of medial orbitofrontal cortex surface area in ADHD ($t = 2.7$, $p = .01$) was similar to a recent finding for autism spectrum disorder. There were also some differences in cortical thickness asymmetry across age groups. In adults with ADHD, globus pallidus asymmetry was altered compared to those without ADHD. However, all effects were small (Cohen's d from −0.18 to 0.18) and would not survive study-wide correction for multiple testing. **Conclusion:** Prior studies of altered structural brain asymmetry in ADHD were likely underpowered to detect the small effects reported here. Altered structural asymmetry is unlikely to provide a useful biomarker for ADHD, but may provide neurobiological insights into the trait. **Keywords:** Attention-deficit; hyperactivity disorder; brain asymmetry; brain laterality; structural MRI; large-scale data.

Introduction

Attention-deficit/hyperactivity disorder (ADHD) is among the most frequently diagnosed childhood-onset mental disorders, affecting 5% of individuals worldwide (Polanczyk, de Lima, Horta, Biederman, & Rohde, 2007). ADHD is characterized by developmentally inappropriate and impairing levels of inattention and/or hyperactivity, impulsivity, and emotional dysregulation (American Psychiatric Association, 2013). At least 15% of children diagnosed with ADHD retain the diagnosis into adulthood (Faraone et al., 2015; Fayyad et al., 2017).

Left-right asymmetry (laterality) is an important feature of human brain organization (Duboc, Dufourcq, Blader, & Roussigne, 2015; Renteria, 2012; Toga & Thompson, 2003), and altered structural or functional asymmetry has been reported for a range of psychiatric conditions (Toga & Thompson, 2003). The right hemisphere is typically dominant for some aspects of attention and arousal (Heilman, Bowers, Valenstein, & Watson, 1986), and it was observed in the 1980s that people with unilateral lesions in the right hemisphere can show ADHD-like symptoms (Heilman et al., 1986). Since then, various neuropsychological and functional imaging studies have found differences between people with ADHD compared to controls (e.g., (Cortese et al., 2012)), with some pointing to a particular involvement of right hemisphere alterations (Geeraerts, Lafosse, Vaes, Vandenbussche, & Verfaillie, 2008; Hale et al.,2010, 2014; Langleben et al., 2001; Stefanatos & Wasserstein, 2001; Vance et al., 2007). However, not all functional data fit a primarily right-hemisphere model (Hale et al., 2009; Mohamed, Börger, Geuze, & van der Meere, 2016; Zou & Yang, 2019).

In terms of brain anatomy, several studies have reported altered asymmetry of the caudate nucleus in ADHD, although not consistently in the direction of effect (Castellanos et al., 1996; Dang et al., 2016; Filipek et al., 1997; Hynd et al., 1993; Schrimsher, Billingsley, Jackson, & Moore, 2002; Uhlikova et al., 2007). Altered asymmetry of gray matter volumes in the superior frontal and middle frontal gyri has been reported in ADHD (Cao et al., 2014), as well as decreased asymmetry of cortical convolution complexity in the prefrontal cortex (X. Li et al., 2007). Reduced hemispheric asymmetry of white matter networks has also been reported in ADHD compared

Conflict of interest statement: See Acknowledgements for full disclosures.

to controls (D. Li et al., 2018). Douglas *et al.* (Douglas et al., 2018) performed the largest study of brain anatomical asymmetry in ADHD to date, including 192 cases with ADHD with a history of pharmacotherapy, 149 medication-naïve cases with ADHD, and 508 typically developing controls (ages 6–-21 years), from eight separate datasets. They calculated per-subject Asymmetry Indexes (AI) for various regional gray matter volumes, AI = (Left-Right)/((Left + Right)/2) (a widely used approach in studies of brain asymmetry (Kong et al., 2018; Kurth, Gaser, & Luders, 2015; Leroy et al., 2015; Postema et al., 2019)), but did not find any significant alterations of AIs in ADHD (Douglas et al., 2018). However, in a subset of their dataset (56 cases and 48 controls), Douglas *et al.* (Douglas et al., 2018) analyzed diffusion tensor imaging (DTI) data, including fractional anisotropy and mean diffusivity measures, and reported alterations in the asymmetry of six white matter tracts, again not specifically driven by alterations in the right hemisphere.

In the current study, we measured cortical regional AIs in 1,978 cases and 1,917 controls from 39 datasets, and subcortical AIs in 1,736 cases and 1,654 controls from 35 datasets, made available via the ADHD working group of the ENIGMA (Enhancing NeuroImaging Genetics through MetaAnalysis) consortium. The same datasets were recently analyzed in two other studies, by Hoogman *et al.*(Hoogman et al., 2017, 2019), that investigated bilateral changes in subcortical volumes and cortical measures, but not alterations of asymmetry. They found that ADHD was associated with lower average volumes of various subcortical structures (Hoogman et al., 2017), as well as lower total and regional cortical surface areas (including frontal, cingulate, and temporal regions), and decreased cortical thickness in fusiform gyrus and temporal pole (Hoogman et al., 2019). These effects were largest in children, and even child-specific for the cortical findings, so that for the present study of asymmetries, we followed the age-group division of Hoogman *et al.* (Hoogman et al., 2019) into children (<15 years), adolescents (15–-21 years), and adults (>21 years), as well as performing analysis in the total combined sample to explore age-general effects. Bilateral effect sizes reported by Hoogman *et al.* (Hoogman et al., 2017, 2019) were small, that is, case–control Cohen's *d* values between −.21 and .06. This suggests that, if associations between ADHD diagnosis and regional brain asymmetries are similarly subtle, many previous studies of anatomical asymmetries in this disorder were underpowered, and the described effects may have been unreliable. Low statistical power in a study not only reduces the chance of detecting true effects, but also the likelihood that significant results reflect true effects (Munafo & Flint, 2010). It is important for the field of neuroimaging to mature around more highly powered analyses in relation to subtle effects. The current study aimed to provide detailed information on the extent to which laterality is affected in ADHD, based on the largest ever sample size for this question, comprised of multiple independent cohorts from around the world.

Methods

Ethical considerations

This study made use of 39 pre-existing datasets from around the world. For all datasets, the participating sites had obtained ethical approval from local institutional review boards, as well as informed consent to participate.

Datasets

Bilateral brain measures derived from structural MRI were available from 39 different datasets via the ENIGMA-ADHD Working Group (Table S1). The 39 datasets comprised cortical data from a total of 1,933 participants with ADHD (1,392 males; median age = 15 y; range = 4 y to 62 y) and 1,829 healthy individuals (1,116 males; median age = 14 y; range = 4 y to 63 y). Subcortical data were available from 35 of the 39 datasets and comprised 1,691 cases (1,212 males, median age = 15 y; range = 5 y to 62 y) and 1,566 controls (953 males, median age = 14 y; range = 4 y to 63 y). A previous study by Douglas *et al.* (Douglas et al., 2018) (see Introduction) included five datasets that were also analyzed in the present study (Table S1).

For all but 4 of the 39 datasets, ADHD diagnosis was based on the Diagnostic and Statistical Manual of Mental Disorders 4th Edition (DSM-IV) (American Psychiatric Association, 2000). Other instruments used were DSM5th Edition (DSM-5), or the International Classification of Diseases (ICD)10th Edition) (World Health Organization, 1992). For information per dataset see, Table S1.

In terms of age groups, for children (<15 y) there were subcortical data from 802 cases and 842 controls, and cortical data from 912 cases and 950 controls; for adolescents (15 y–21 y) there were subcortical data from 326 cases and 232 controls, and cortical data from 408 cases and 340 controls; for adults (> 21 years) there were subcortical data from 563 cases and 492 controls, and cortical data from 613 cases and 539 controls.

Eleven additional datasets, comprising cases-only or controls-only, were excluded for the purpose of the present study (these are not listed in Table S1). This was because our analysis models included random intercepts for 'dataset' (below), and diagnosis would be fully confounded with 'dataset' for case-only or control-only datasets.

MRI-based measures

Structural T1-weighted brain MRI scans had been acquired at each study site for each of the 39 pre-existing MRI datasets. MRI data within the ENIGMA consortium are typically processed separately at each participating site, due to varying restrictions on data sharing that apply to the many legacy datasets from different countries around the world. Images were obtained at different field strengths (1.5 T or 3 T: see Table S1). Scanners and scanning sequences, recruitment criteria, and demographics differed between datasets, but all sites separately applied a single image processing and quality control protocol from the ENIGMA consortium (http://enigma.ini.usc.edu/protocols/imaging-protocols), starting from their T1 image data. The harmonized processing was based on the freely available and validated software FreeSurfer (versions 5.1 or 5.3) (Fischl, 2012), with the default 'recon-all' pipeline (https://surfer.nmr.mgh.harvard.edu/fswiki/recon-all), which is a 29-step procedure that includes skull stripping,

registration, subcortical segmentation, normalization, white matter and pial surface creation, cortical parcellation according to the Desikan-Killiany atlas, and the output of region-specific measures of volume, average thickness, and surface area. This was followed by visual inspection of both internal and external segmentations (Supplementary Methods). Exclusions on the basis of these quality control steps resulted in the sample sizes given above. The present study took as its starting point the FreeSurfer-derived measures of left and right volumes of seven bilaterally paired subcortical structures, and thickness and surface area measures for each of 34 bilaterally paired cortical regions, that were generated previously by each site. The cortical regions were defined by the Desikan-Killiany atlas (Desikan et al., 2006). In addition, the average cortical thickness and total surface area per hemisphere were analyzed. FreeSurfer's measure of intracranial volume (ICV) was also considered as a covariate in sensitivity analyses (below).

The Desikan-Killiany atlas (Desikan et al., 2006) was derived from manual segmentations of reference brain images. The labeling system incorporates hemisphere-specific information on sulcal and gyral geometry with spatial information regarding the locations of brain structures (Desikan et al., 2006). Accordingly, the mean regional asymmetries in our data might be influenced by left-right differences present in the reference dataset used for constructing the atlas. Nonetheless, this approach was appropriate for our study focused on comparing relative asymmetry between groups. The use of an asymmetrical atlas has the advantage that regional identification is likely to be accurate for structures that are asymmetrical both in the atlas and, on average, in the study population.

Asymmetry indexes

Left and right data per brain region and individual participant were loaded into R (version 3.5.3), and null values were removed. An asymmetry index (AI) was calculated for each subject and each paired left-right measure using the following formula: (Left-Right)/(Left + Right). Negative AIs therefore indicate a right > left asymmetry, while positive AIs indicate a left > right asymmetry. In the AI formula, the L-R difference (numerator) is adjusted by the bilateral measure L + R (denominator), such that the AI does not scale with the bilateral measure. We did not divide the denominator by 2, in contrast to some previous formulations of AIs (see Introduction), but this makes no difference in terms of deriving Cohen's *d* effect sizes and *p*-values for group comparisons. Distributions of each of the AIs in the total study sample are plotted in Figure S1.

Correlations between AI measures in the total study sample were calculated using Pearson's R and visualized using the *corrplot* package in R (Figures S2–S4). Most pairwise correlations between AIs were of low magnitude (median magnitude $r = .024$ for surface area AIs, 0.040 for thickness AIs, 0.091 for subcortical volume AIs), with a minimum $r = -.42$ between caudal anterior cingulate surface area and superior frontal surface area, and maximum $r = .49$ between rostral middle frontal thickness and total average thickness.

Linear mixed effects random-intercept models

Main analysis. Linear mixed effects analyses were performed separately for each subcortical volume AI, cortical regional surface and thickness AI, and the total hemispheric surface area, and average thickness AI, using the *nlme* package in R (version 3.5.3). Analyses were conducted separately within children, adolescents, and adults, as well as on the total study sample. All models included *diagnosis* (a binary variable; 0 = control, 1 = case), *sex* (binary; 0 = female, 1 = male), and *age* (numeric) as fixed factors, and *dataset* as a random factor (39 categories for cortical data, 35 categories for subcortical data):

$$AI\ diagnosis + sex + age + random(\ 1|dataset) \quad (1)$$

The maximum likelihood (ML) method was used to fit the models. Whenever any of the predictor variables was missing in a given subject, the subject was omitted from the analysis (method = 'na.omit'). The 'optim' optimizer (lmeControl(opt='optim') was used for all models. Residual plots are in Figures S5–S7.

The t-statistic for the factor 'diagnosis' in each linear mixed effects model was derived and used to calculate Cohen's *d* (Supplementary Methods). For visualization of cerebral cortical results, Cohen's *d* values were loaded into Matlab (v. R2020a) and 3D images of left hemisphere inflated cortical and subcortical structures were obtained using FreeSurfer-derived ply files.

Field strength was not included as a covariate because each dataset was scanned entirely at either 1.5 T or 3T (Table S1), and the models included 'dataset' as a random-intercept effect, which adjusted for differences that applied to entire datasets.

Significance and detectable effect sizes. Significance was assessed based on the *p*-value for the diagnosis term within each model. Separately within each age group, and again within all age groups combined, we applied false discovery rate (FDR) correction (Benjamini & Hochberg, 1995) for multiple testing, separately across the seven subcortical structures, the 35 cortical surface area AIs (i.e., 34 regional AIs and one hemispheric total AI), and again for the 35 cortical thickness AIs, each time with an FDR threshold of 0.05. Therefore, twelve separate FDR corrections were done. We also applied an additional FDR correction for the total combined analysis across all age groups and AIs of different types.

As each linear model included multiple predictor variables, the power to detect an effect of diagnosis on AI could not be computed exactly, but we obtained an indication of the effect size that would be needed to provide 80% power had we been using simple t-tests and Bonferroni correction for multiple testing, using the *pwr* command in R (Supplementary Methods). For this purpose, a significance level of 0.0071 (i.e., 0.05/7) or 0.0014 (i.e., 0.05/35) was set in the context of multiple testing over the seven subcortical volumes, or the regional and total cortical surface areas ($N = 35$) or thicknesses ($N = 35$). This showed that, in the total study sample, a case–control effect size of roughly Cohen's $d = .12$ (subcortical), or $d = .13$ (cortical), would be detectable with 80% power. For the analyses in the different age groups, this was, respectively, $d = .16$ and $d = .19$ in children, $d = .26$ and $d = .30$ in adolescents, and $d = .21$ and $d = .24$ in adults.

Directions of asymmetry changes. For any AIs showing nominally significant effects (i.e., unadjusted $p < .05$) of diagnosis in any of the primary analyses, *post hoc* linear mixed effects modeling was also performed on the corresponding L and R measures separately, to understand the unilateral changes involved. The models included the same terms as were used in the main analysis of AIs (i.e., diagnosis, age and sex as fixed factors, and dataset as random factor). Again, the Cohen's *d* effect sizes for diagnosis were calculated based on the *t*-statistics. The raw mean AI values were calculated separately in controls and cases, to describe the reference direction of healthy asymmetry in controls, and whether cases showed lower, higher, or reversed asymmetry relative to controls.

Sensitivity analyses. The relationships between AIs and age appeared roughly linear across all age groups combined (Figures S8–S10). Therefore, no polynomials for age were

incorporated in the main model (Supplementary Methods). However, analyses were repeated (only for all age groups combined) using an additional nonlinear term for age, to check whether this choice had affected the results. The variables age and age^2 are inevitably highly correlated. To include linear and nonlinear effects of age in the same model, we made use of the poly()-function in R for these two predictors, which created a pair of uncorrelated variables related to age (so-called orthogonal polynomials) (Chambers & Hastie, 1992), where one variable was linear and one nonlinear:

$$AI\ diagnosis + poly(age, 2) + sex + random(\ 1|dataset) \quad (2)$$

Note that we were not interested to measure the effects of age or age-squared, but simply to correct for linear and nonlinear effects related to age, as we measured the effects of diagnosis on brain asymmetry.

No AI outliers were removed for the main analysis, but to confirm that results were not dependent on outliers, the main analysis was also repeated (for all age groups combined) after having winsorized using a threshold of $k = 3$, for each AI measure separately in the total combined dataset.

Associations between brain asymmetries and IQ, comorbidity, ADHD severity, and psychostimulant medication. Within the ADHD participants only (all age groups combined), brain asymmetries were tested in relation to several potentially associated variables (IQ, comorbidity, severity, medication use; see Figures S11 and S12), using separate models in which each variable was considered as a fixed effect:

$$AI\ variable + age + sex + random(\ 1|dataset) \quad (3)$$

See Supplementary Methods for the derivation of these variables. For binary variables, datasets were removed if they had < 1 subject per category, to avoid the random variable 'dataset' being fully confounded with the binary variable for any datasets. Depending on the availability of each specific AI, data for testing association with IQ were available for up to 1,719 ADHD individuals (exact numbers per AI depended on image quality control for that region and can be found in the relevant results tables, see below). For the presence/absence of comorbidities, four different binary variables were constructed: mood disorder (up to 179 yes, 384 no), anxiety disorder (up to 82 yes, 503 no), oppositional defiant disorder (ODD; up to 80 yes, 151 no), and substance use disorder (SUD; up to 77 yes, 335 no). For ADHD symptom severity, two continuous variables were used: hyperactivity/impulsivity (up to 1,009 ADHD participants) and inattention (1,006 ADHD participants). For psychostimulant medication use, two binary variables were constructed: lifetime use (up to 337 yes, 188 no), and current use (i.e., at the time of scanning, up to 361 yes, 377 no) (see Figures S12 for the distributions, and Supplementary Methods for more explanation).

IQ was also examined in controls-only (all age groups combined) to explore the relationships between IQ and brain asymmetries in typically developing individuals. IQ and AI data were available for up to 1,663 controls. The model for each AI was:

$$AI\ IQ + age + sex + random(\ 1|dataset).$$

IQ, handedness, and intracranial volume as covariates in disorder case–control analysis. See the Supporting Information for the derivation of IQ and handedness measures, and above for ICV. Distributions are in Figures S11. We did not adjust for IQ, handedness, or ICV as covariate effects in our main, case–control analysis (above). This was because, *a priori*, there are various possible causal relations linking these traits to ADHD and brain asymmetry and other, possibly underlying factors shared between some or all of them. In this context, it is important not to bias associations between ADHD and brain asymmetry through correcting for these factors as covariates in primary analysis, as they may be colliders (Cole et al., 2010) (see the Discussion for more on this issue). However, we included a set of additional, secondary models to test for case–control effects in the presence of these variables as covariates:

AI ~ diagnosis + age + sex + + handedness + random (~1 | dataset)
*AI ~ diagnosis + age + sex + handedness + handedness*diagnosis + random (~1 | dataset)*
AI ~ diagnosis + age + sex + IQ + random (~1 | dataset)
*AI ~ diagnosis + age + sex + IQ + IQ*diagnosis + random (~1 | dataset)*
AI ~ diagnosis + age + sex + + ICV + random (~1 | dataset)
*AI ~ diagnosis + age + sex + ICV + ICV*diagnosis + random (~1 | dataset)*

The analyses were also repeated after winsorization of outliers, as above.

Results

Associations of brain asymmetry with ADHD

Results for all AIs across the different age groups, and for all age groups combined, are listed in the supplement (Tables S2–S13), and are also available as supplementary comma-delimited text files.

Children. There were no associations of diagnosis with AIs that had FDR < 0.05 in children (Tables 1–3, Tables S2–S4). The children showed nominally significant associations (unadjusted $p < .05$) of diagnosis with the AIs of total hemispheric surface area ($t = 2.10$, $p = .036$), medial orbitofrontal cortex surface area ($t = 2.7$, $p = .006$), and paracentral lobule surface area ($t = -2.16$, $p = .031$) (Table 1, Table S3). The Cohen's d for these effects were .11, .13 and −.10, respectively (Figure 1, Figures S13, Table S3). *Post hoc* analysis showed that the effects on total hemispheric and medial orbitofrontal surface area asymmetries both involved relatively greater reductions on the right-side than left-side in ADHD compared to controls (Table S14). The effect on paracentral lobule surface area asymmetry was driven by a larger decrease of left compared to right-hemispheric surface area in this region (Table S14).

The children also showed nominally significant associations of diagnosis with four regional cortical thickness AIs, which were the banks of the superior temporal sulcus ($t = -2.0$, $p = .047$; increased rightward asymmetry in ADHD), caudal middle frontal cortex ($t = 2.1$, $p = .037$; increased leftward asymmetry), precentral gyrus ($t = 2.4$, $p = .019$; increased leftward asymmetry) and insula ($t = -2.0$, $p = .047$, decreased leftward asymmetry) (Table 2, Table S14).

Adolescents. There were two nominally significant associations between diagnosis and AIs in

Table 1 Linear mixed model results for subcortical volume AIs

	Children only		Adolescents only		Adults only		Total study sample	
Subcortical volume AI	p^a	d^b	p^a	d^b	p^a	d^b	p^a	d^b
Accumbens	.26	−.06	.36	−.08	.90	.01	.32	−.03
Amygdala	.78	−.01	.72	.03	.69	−.03	.61	−.02
Caudate Nucleus	.60	.03	.88	.01	.45	.05	.41	.03
Globus Pallidus	.65	−.02	.39	−.08	***.004***	−.18	**.01**	−.09
Hippocampus	.84	−.01	.09	.15	.46	.05	.62	.02
Putamen	.54	−.03	.87	−.02	.52	−.04	.26	−.04
Thalamus	.42	.04	.28	.10	.48	.04	.15	.05

[a]Uncorrected *p*-values for diagnosis are indicated, with in bold those that are significant at the uncorrected level ($p < 0.05$), and in bold-italic those that survive multiple testing correction within the particular analysis indicated (see text).
[b]Cohen's *d* value for the effect of diagnosis.

adolescents, but none with FDR < 0.05 (Tables 1–3, Tables S5–S7). These involved the *pars orbitalis* of inferior frontal gyrus surface area ($t = 2.4$, $p = .017$), which showed lower rightward asymmetry in ADHD compared to controls, due to a smaller left than right-sided decrease (Table S14), and cuneus thickness ($t = -2.0$, $p = .043$), which showed greater rightward asymmetry in ADHD compared to controls, due to an increase in right- and a decrease in left-hemispheric thickness (Table S14).

Adults. In adults, the globus pallidus AI was significantly associated with ADHD diagnosis with FDR < 0.05 ($t = -2.9$, $p = .004$, uncorrected) (Table 1, Table S8). The Cohen's *d* effect size for this association was −.18 (Table 1, Figure 1, Figure S13). This effect involved a decrease in leftward asymmetry in ADHD compared to controls, driven by a larger reduction of left-side volume than right-side volume in ADHD compared to controls (Table S14). Note this association was only significant in the context of FDR correction for 7 subcortical AIs within adults specifically. (No effects were significant at FDR-corrected $p < .05$ when the correction was done across all age groups and AIs of different types, see below).

There were other nominally significant associations of AIs with diagnosis in adults: lateral occipital cortex surface area ($t = 2.0$, $p = .049$; increased leftward) (Table 2, Tables S9 and S14) and thickness ($t = 2.2$, $p = .026$; decreased rightward) (Table 3, Tables S10 and S14), medial orbitofrontal cortex thickness ($t = 2.0$, $p = .045$; increased leftward), middle temporal gyrus thickness ($t = -2.6$, $p = .009$; increased rightward), pericalcarine cortex thickness ($t = 2.9$, $p = .004$; decreased rightward), and postcentral gyrus thickness ($t = -2.5$, $p = .013$; decreased leftward). The corresponding unilateral effects are shown in Table S14.

All age groups combined. When combining all age groups, there were nominally significant associations of AIs with diagnosis for the medial orbitofrontal cortex surface area ($t = 2.2$, $p = .029$; decreased rightward), paracentral lobule surface area ($t = -2.2$, $p = .029$; increased rightward), pars orbitalis of inferior frontal gyrus surface area ($t = 2.3$, $p = .021$; decreased rightward), caudal middle frontal thickness ($t = 2.2$, $p = .027$; increased leftward), insula thickness ($t = -2.1$, $p = .040$; decreased leftward), as well as the volume of the globus pallidus ($t = -2.6$, $p = .010$; decreased leftward) (Tables 1–3, Tables S11–S13). The corresponding unilateral effects are shown in Table S14.

No effects were significant at FDR-corrected $p < .05$ when the correction was done across all age groups and AIs of different types.

The addition of nonlinear effects of age to the model had negligible influences on the six nominally significant associations with diagnosis, all of which remained nominally significant except insula thickness (now $p = .050$). Likewise, winsorizing outliers (using a threshold $k = 3$, see Methods) also had little influence on the results (the effect on insula thickness asymmetry was no longer nominally significant, $p = .061$) (Tables S15–S17).

Associations brain asymmetries with comorbidity, ADHD severity, psychostimulant medication, and IQ

Analyses in this section were carried out in all age groups combined.

When testing associations of comorbidity, ADHD severity, psychostimulant medication, or IQ with brain asymmetries within ADHD individuals (Tables S18–S29), only one significant association was found (FDR < 0.05 within the particular type of AI and age-defined group), namely between comorbid mood disorder and the rostral middle frontal gyrus thickness AI ($p = .0002$, $t = 3.70$) (Table S26). Furthermore, various nominally significant ($p < .05$) associations were observed: ADHD severity was associated with the AI of the entorhinal cortex surface area ($t = 2.12$, $p = .034$; hyperactivity/impulsivity) (Table S19). ADHD severity was also associated with four regional cortical thickness

Table 2 Linear mixed model results for the cortical surface area AIs

Cortical surface area AI	Children only		Adolescents only		Adults only		Total study sample	
	p^a	d^b	p^a	d^b	p^a	d^b	p^a	d^b
Banks of superior temporal sulcus	.80	−.01	.53	−.05	.81	.01	.48	−.02
Caudal anterior cingulate cortex	.75	−.01	.29	−.08	.71	.02	.64	−.02
Caudal middle frontal cortex	.41	.04	.55	−.05	.22	.07	.19	.04
Cuneus	.16	.07	.92	−.01	.07	−.11	.74	−.01
Entorhinal cortex	.95	.003	.42	−.06	.10	−.10	.34	−.03
Frontal pole	.05	−.09	.22	.09	.25	−.07	.10	−.05
Fusiform gyrus	.17	−.06	.35	.07	.11	−.10	.15	−.05
Inferior parietal cortex	.27	.05	.98	−.002	.89	−.01	.44	.03
Inferior temporal gyrus	.57	.03	.84	.02	.25	.07	.25	.04
Insula	.10	.08	.56	.04	.64	−.03	.28	.04
Isthmus cingulate cortex	.95	−.003	.19	−.10	.49	.04	.75	−.01
Lateral occipital cortex	.59	−.02	.96	−.004	.05	.12	.48	.02
Lateral orbitofrontal cortex	.18	−.06	.54	−.05	.42	−.05	.06	−.06
Lingual gyrus	.88	−.01	.14	−.11	.50	.04	.92	−.003
Medial orbitofrontal cortex	**.01**	.13	.27	.08	.72	−.02	**.03**	.07
Middle temporal gyrus	.15	.07	.45	−.06	.89	−.01	.38	.03
Paracentral lobule	**.03**	−.10	.96	−.004	.28	−.06	**.03**	−.07
Parahippocampal gyrus	.37	.04	.25	−.09	.13	−.09	.73	−.01
Pars opercularis of inferior frontal gyrus	.88	.01	.19	.10	.58	.03	.34	.03
Pars orbitalis of inferior frontal gyrus	.20	.06	**.02**	.18	.55	.04	.02	.08
Pars triangularis of inferior frontal gyrus	.32	.05	.14	.11	.57	−.03	.24	.04
Pericalcarine cortex	.30	.05	.13	−.12	1.00	.00	.94	.002
Postcentral gyrus	.44	.04	.29	.08	.98	.00	.39	.03
Posterior cingulate cortex	.62	−.02	.46	−.06	.84	.01	.59	−.02
Precentral gyrus	.85	.01	.09	−.13	.05	−.12	.09	−.06
Precuneus	.29	.05	.47	−.06	.65	.03	.46	.02
Rostral anterior cingulate cortex	.97	−.002	.98	.002	.36	−.05	.51	−.02
Rostral middle frontal gyrus	.10	−.08	.77	−.02	.60	−.03	.11	−.05
Superior frontal gyrus	.28	.05	.09	.13	.11	−.09	.55	.02
Superior parietal cortex	.09	.08	.33	.07	.68	−.02	.27	.04
Superior temporal gyrus	.09	.08	.87	.01	.19	−.08	.62	.02
Supramarginal gyrus	.86	.01	.25	−.09	.21	−.07	.24	−.04
Temporal pole	.65	.02	.69	.03	.34	−.06	.97	.001
Transverse temporal gyrus	.66	−.02	.44	.06	.94	.005	.93	.003
Total average surface area	**.04**	.10	.73	.03	.23	−.07	.54	.02

[a]Uncorrected *p*-values for diagnosis are indicated, with in **bold** those that are significant at the uncorrected level ($p < .05$). None survived multiple testing correction.
[b]Cohen's *d* value for the effect of diagnosis.

asymmetries: the caudal anterior cingulate thickness AI ($t = 2.66$, $p = .008$; hyperactivity/impulsivity), *pars opercularis* of the inferior frontal gyrus thickness AI ($t = 2.12$, $p = .034$; hyperactivity/impulsivity, and $t = 2.04$, $p = .04$; inattention), and pericalcarine cortex thickness AI ($t = 2.04$, $p = .04$; hyperactivity/impulsivity) (Table S20).

Current psychostimulant medication use was associated with two cortical regional surface area asymmetries, that is, precuneus ($t = -2.25$, $p = .025$) and transverse temporal gyrus ($t = -2.34$, $p = .020$) (Table S22), and with two thickness asymmetries, that is, inferior parietal cortex ($t = -2.33$, $p = .020$) and precentral gyrus ($t = -2.16$, $p = .031$) (Table S23). Lifetime psychostimulant medication use was associated with three cortical surface area asymmetries (insula ($t = -2.03$, $p = .043$), supramarginal gyrus ($t = -2.08$, $p = .038$), and rostral anterior cingulate cortex ($t = 1.97$, $p = .049$) (Table S22), and the thickness asymmetry of the paracentral lobule ($t = 2.15$, $p = .032$) (Table S23). Among the AIs which showed nominally significant associations with medication use, one had also shown a nominally significant association with diagnosis in all age groups combined, that is, the AI of paracentral lobule surface area (see above). The direction of medication effect was positive, that is, the opposite to the effect of diagnosis on this AI (see above).

For mood disorder, associations were observed with six thickness AIs (i.e., entorhinal cortex, pars triangularis of inferior frontal gyrus, pericalcarine cortex, precuneus, rostral middle frontal gyrus, and transverse temporal gyrus), and two surface area AIs (i.e., inferior temporal gyrus, and rostral anterior cingulate cortex), of which the association with rostral middle frontal thickness AI survived multiple testing correction (FDR < 0.05) (Tables S5 and S26).

Table 3 Linear mixed model results for the cortical thickness AIs

	Children only		Adolescents only		Adults only		Total study sample	
Cortical thickness AI	p^a	d^b	p^a	d^b	p^a	d^b	p^a	d^b
Banks of superior temporal sulcus	.05	−.10	.54	−.05	.64	−.03	.06	−.06
Caudal anterior cingulate cortex	.25	.05	.60	−.04	.06	.11	.11	.05
Caudal middle frontal cortex	**.04**	.10	.09	.13	.73	.02	**.03**	.07
Cuneus	.69	.02	**.04**	−.15	.06	.11	.56	.02
Entorhinal cortex	.12	−.08	.79	.02	.65	−.03	.26	−.04
Frontal pole	.27	.05	.20	−.10	.19	.08	.34	.03
Fusiform gyrus	.56	−.03	.98	.002	.79	.02	.94	−.003
Inferior parietal cortex	.96	.00	.59	−.04	.51	.04	.81	.01
Inferior temporal gyrus	.24	−.05	.79	.02	.84	−.01	.69	−.01
Insula	.05	−.09	.32	−.08	.94	−.004	.05	−.06
Isthmus cingulate cortex	.81	−.01	.22	.09	.35	−.06	.91	.00
Lateral occipital cortex	.76	.01	.40	−.06	**.03**	.13	.41	.03
Lateral orbitofrontal cortex	.75	−.01	.51	.05	.14	.09	.42	.03
Lingual gyrus	.34	−.04	.85	.01	.59	−.03	.29	−.04
Medial orbitofrontal cortex	.06	−.09	.31	.08	.04	.12	.97	.001
Middle temporal gyrus	.75	−.02	.62	−.04	.01	−.17	.11	−.05
Paracentral lobule	.15	−.07	.12	.12	.77	−.02	.53	−.02
Parahippocampal gyrus	.07	−.09	.09	−.13	.39	.05	.12	−.05
Pars opercularis of inferior frontal gyrus	.80	.01	.39	.07	.89	−.01	.45	.02
Pars orbitalis of inferior frontal gyrus	.36	.04	.95	−.004	.37	.05	.30	.03
Pars triangularis of inferior frontal gyrus	.67	−.02	.36	.07	.90	−.01	.92	.003
Pericalcarine cortex	.92	−.004	.98	−.002	**.004**	.17	.15	.05
Postcentral gyrus	.94	−.004	.92	−.01	**.01**	−.15	.11	−.05
Posterior cingulate cortex	.57	−.03	.47	−.05	.87	−.01	.35	−.03
Precentral gyrus	**.02**	.11	.32	−.08	.17	.08	.05	.06
Precuneus	.73	.02	.22	.09	.69	.02	.36	.03
Rostral anterior cingulate cortex	.92	−.004	.06	.15	.36	.06	.21	.04
Rostral middle frontal gyrus	.68	.02	.78	−.02	.34	−.06	.85	−.01
Superior frontal gyrus	.77	.01	.10	.13	.64	.03	.30	.03
Superior parietal cortex	.98	−.001	.47	−.06	.85	.01	.77	−.01
Superior temporal gyrus	.06	.09	.42	.07	.36	−.06	.28	.04
Supramarginal gyrus	.18	−.06	.51	−.05	.93	−.005	.19	−.04
Temporal pole	.56	.03	.77	.02	.62	−.03	.77	.01
Transverse temporal gyrus	.66	.02	.65	.03	.34	−.06	.98	−.001
Total average thickness	.92	−.005	.78	.02	.75	.02	.78	.01

[a]Uncorrected *p*-values for the effects of diagnosis are indicated, with in **bold** those that are significant at the uncorrected level ($p < .05$). None of the associations with diagnosis survived multiple testing correction.
[b]Cohen's *d* value for the effect of diagnosis.

Anxiety Disorder was associated with thickness AIs of the cuneus and lateral occipital cortex (Table S26). For ODD, associations were found with the AIs of medial orbitofrontal thickness (Table S26) and temporal pole surface area (Table S25). Additionally, SUD was associated with the thickness AIs of the cuneus and paracentral lobule (Table S26), and with surface area AIs of the postcentral gyrus and supramarginal gyrus (Table S25). None of these regions showed a nominally significant effect of diagnosis in the main analysis of all age groups combined.

Finally, within ADHD individuals, IQ was nominally associated with the accumbens volume AI ($t = 2.16$, $p = .031$), hippocampus volume AI ($t = -2.06$, $p = .039$) (Table S27), and lateral occipital cortex surface area AI ($t = -2.17$, $p = .030$) (Table S28). Within controls, IQ was associated with the middle temporal gyrus surface area AI ($t = -2.52$, $p = .012$) (Table S28), rostral anterior cingulate thickness cortex AI ($t = 2.47$, $p = .014$), and supramarginal gyrus thickness AI ($t = -2.55$, $p = .011$) (Table S29).

Including IQ, handedness, or intracranial volume as covariates in case–control analysis. We carried out secondary analyses in which IQ, handedness, or intracranial volume were included as covariates in case–control analysis, with or without interaction terms for these variables with diagnosis (i.e., case–-control status) (see Methods for the models used). These extra models identified a small number of main effects of diagnosis, or interactions with diagnosis, that survived multiple testing correction at FDR < 0.05 within the specific subset of AIs and ages being analyzed (but would not survive further correction for multiple testing). However, after winsorization of outliers (see Methods), only the diagnosis term for globus pallidus volume AI remained

significant, in the model *AI ~ diagnosis + age + sex + ICV + random (~1|dataset)*, when analyzed in the total study sample ($p = .005$, $t = -2.75$), or when analyzed in adults only ($p = .0035$, $t = -2.93$). Complete model results from all of these secondary analyses can be found in supplementary comma-delimited text files.

Discussion

We conducted the largest study to date of associations between anatomical brain asymmetries and ADHD. Linear mixed effects model mega-analyses were carried out separately in children, adolescents, and adults, following previous ENIGMA-ADHD working group studies of bilateral brain differences that showed contrasting effects in these age groups (Hoogman et al., 2017, 2019). We also analyzed the total study sample for age-general effects. All statistical effects of diagnosis on asymmetries were very small, with Cohen's *d* ranging from −.18 to .18. Only one of these associations was significant with a false discovery rate < 0.05 within the specific subset of AIs and age-defined subjects in which it was found (globus pallidus asymmetry in adults), and this effect was not significant in analysis of all age groups combined, with FDR correction across all AIs. Therefore, all effects remain tentative, even in this unprecedented sample size. The small effect sizes mean that altered brain asymmetry is unlikely, in itself, to be a useful biomarker or clinical predictor of ADHD. In addition, our results suggest that significant effects reported in prior studies, based on much smaller samples, may have been unrealistically large. As noted in the Introduction, low power not only reduces the chance of detecting true effects, but also increases the likelihood that statistically significant results do not reflect true effects (Munafo & Flint, 2010). There were some notable associations of diagnosis with cortical asymmetry that reached nominal significance in our study. Among these, children with ADHD showed reduced rightward asymmetry of total hemispheric surface area and medial orbitofrontal surface area. In a recent ENIGMA consortium study of autism spectrum disorder (ASD), medial orbitofrontal cortex surface area asymmetry was altered in the same direction, and to a similar extent, as in the present study (Postema et al., 2019). ADHD and ASD often co-occur (Leitner, 2014) and are known to share genetic influences (Ghirardi et al., 2019; Stergiakouli et al., 2017), such that the two diagnostic labels are likely to capture a partly overlapping spectrum of related disorders (Demopoulos, Hopkins, & Davis, 2013; van der Meer et al., 2012). Studies that aimed to identify shared brain structural traits between ADHD and ASD have found mixed results (Boedhoe et al., 2019; Radonjić et al., 2019), with perhaps the greatest overlap involving regions of the 'social brain', including orbitofrontal cortex (Baribeau et al., 2019). However, laterality has not been specifically studied in this regard, so that our finding of reduced rightward medial orbitofrontal cortex surface area in both disorders may be a new insight into shared neurobiology between ADHD and ASD. Altered lateralized neurodevelopment may play a causal role in disorder susceptibility, or else may arise as a correlated trait due to other underlying susceptibility factors, or even be a downstream consequence of having the disorder (Bishop, 2013). Some aspects of brain asymmetry are partly heritable (Guadalupe et al., 2016; Kong et al., 2018), so that future gene mapping studies for brain asymmetry and disorder susceptibility may help to resolve causal relations underlying their associations.

One functional imaging study (94 cases, 85 controls) reported lower rightward lateralization in medial orbitofrontal cortex in ADHD compared to controls, based on temporal variability during resting-state (Zou & Yang, 2019). Furthermore, a study of 218 participants with ADHD and 358 healthy controls reported that orbitofrontal cortex thickness, but not surface area, showed a left > right asymmetry in childhood controls that switched to right > left asymmetry by late adolescence, while this change did not occur to the same extent in ADHD (Shaw et al., 2009). However, in the present study, there was no effect of diagnosis on thickness asymmetry of this region in children or adolescents, while in adults, ADHD was associated with a relatively rightward shift of asymmetry compared to controls, that is, opposite to what might be expected according to Shaw *et al*. For other cortical asymmetries too, our findings in this large-scale study were discrepant with what might have been expected from previous reports in smaller samples (see references in the Introduction). For example, a prior study reported reversed gray matter volume asymmetry (i.e., leftward instead of rightward) of the superior frontal gyrus in ADHD (Cao et al., 2014), but we saw no clear evidence of this in the present study.

The most often reported alteration of brain asymmetry in ADHD has involved the caudate nucleus, although the direction of the effect has not been consistent (Castellanos et al., 1996; Dang et al., 2016; Filipek et al., 1997; Hynd et al., 1993; Schrimsher et al., 2002; Uhlikova et al., 2007). We did not find evidence for altered asymmetry of caudate nucleus volume in the present study, again suggesting that prior findings were false positives in smaller samples. As mentioned above, we found a tentative association with ADHD for another regional asymmetry of the basal ganglia, namely of the globus pallidus, in adults-only. The globus pallidus is involved in movement and reward processing (Munte et al., 2017), both of which are involved in the symptomatology of ADHD. A previous meta-analysis comprising data from a total of 114 participants with ADHD (or a related disorder) and 143 control

participants, noted a significantly lower average right putamen and right globus pallidus volumes in ADHD (Ellison-Wright, Ellison-Wright, & Bullmore, 2008), although asymmetry was not quantified in that study. Regardless, our finding of lower leftward asymmetry seems discrepant with this earlier report.

We have already remarked on the limited statistical power of previous studies as a likely explanation for their findings being discrepant with the current study. Low sample sizes in relation to subtle effects can result in poor reproducibility (Button et al., 2013; Munafo & Flint, 2010). Here, we had 80% power to detect case–control Cohen's *d* effect sizes as low as roughly .12, or as high as 0.3 in the smallest subset by age (see Methods). In addition to limited sample sizes, there are various other possible explanations for discrepancies with previous studies. Methodological differences in hardware, software, and data processing pipelines can influence results (Biberacher et al., 2016), although our focus on asymmetry through use of the AI is likely to have reduced the impact of heterogeneity factors that affect both hemispheres equally. In contrast to some previous studies mentioned above, we did not consider gyral/sulcal patterns or cortical gray matter volumes as such. Rather, we studied regional cortical thicknesses and surface areas as distinct measures, which together drive gray matter volumetric measures. Since area and thickness have been shown to vary relatively independently (Panizzon et al., 2009), separate analyses are advisable, although cortical thickness measures are particularly prone to effects related to site-, scanner- or protocol differences (Chung et al., 2017; Fortin et al., 2018). Likewise, the choice of brain atlas can influence results, as each atlas has its own properties that impact brain segmentation (Yaakub et al., 2020). In addition, the approach we used is based on hemisphere-specific definitions of regional anatomy, because each hemisphere has its own atlas, based on its own average distribution of features (Desikan et al., 2006). Correspondence between hemispheres is then achieved at the regional level, based on expert neuroanatomical regional segmentation that was adapted to each hemisphere's distinct features when constructing the atlas. However, future studies using higher-resolution atlases, or vertex-based analysis using hemispheric co-registration (Kang, Herron, Cate, Yund, & Woods, 2012; Maingault, Tzourio-Mazoyer, Mazoyer, & Crivello, 2016), may identify restricted regions showing stronger associations between ADHD and cortical asymmetry than we report here. Furthermore, for subcortical volume asymmetries, discrepancies between the findings of our study and previous studies could be due to differences in parcellation methods, which can perform with varying accuracy (Guadalupe et al., 2014; Pardoe, Pell, Abbott, & Jackson, 2009; Perlaki et al., 2017).

The conceptualization of laterality can also differ across studies. In terms of AIs, our cortical results are largely in line with a previous report based on measuring gray matter volume asymmetries in 192 participants with ADHD and 508 controls (Douglas et al., 2018), insofar as no FDR-significant results were found (five of those datasets were in common with the present study, see Methods). However, the authors of that study also calculated the unsigned magnitudes of the AIs (i.e., absolute degrees of asymmetry, regardless of directions). They reported significant differences in absolute asymmetry for various cortical and subcortical structures (Douglas et al., 2018). In the present study, we did not calculate absolute AIs, in order not to compound multiple testing, and because these measures are highly non-normal with a floor effect at value zero, which would violate the assumptions of the modeling that we applied. It is not clear whether this issue may have affected the results in the earlier study (Douglas et al., 2018). Future studies may consider the unsigned magnitude of brain asymmetry indexes further in ADHD, but it will be necessary to use statistical methods that can account for non-normal distributions.

Discrepancies with earlier studies may also be due to differences in clinical features of the disorder that arise from case recruitment and diagnosis, for example with respect to medication use (which has been suggested to partly normalize brain structural abnormalities, although the previous ENIGMA studies of bilateral changes in ADHD did not support this) (Nakao, Radua, Rubia, & Mataix-Cols, 2011; Pretus et al., 2017), comorbidities (Reale et al., 2017), symptom severity, and/or IQ. Some asymmetries showed tentative associations with some of these clinical variables in the present study, although none of these results survived correction for multiple testing, apart from mood disorder with the rostral middle frontal thickness AI. Also, some of the clinical variables (medication, comorbidity) were missing for many ADHD individuals in this study. Regardless, it remains possible that certain subsets of ADHD might be associated more strongly with altered brain asymmetry than was apparent in our large-scale analysis of average changes over many datasets, comprising many and varied collections of ADHD individuals and controls.

In general, between-center heterogeneity (in terms of scanning setup, patient subgroups, demographics) may result in reduced statistical power to detect effects that are specific to certain subgroups of datasets, or to individual datasets, when tested in mega-analysis over all datasets. For example, harmonization of scanning protocols might lead to stronger effects being found, as heterogeneity of this aspect would be reduced. Here, we used random-intercept models to adjust for heterogeneity between datasets. This was a strong correction for cross-dataset heterogeneity, as it removed mean

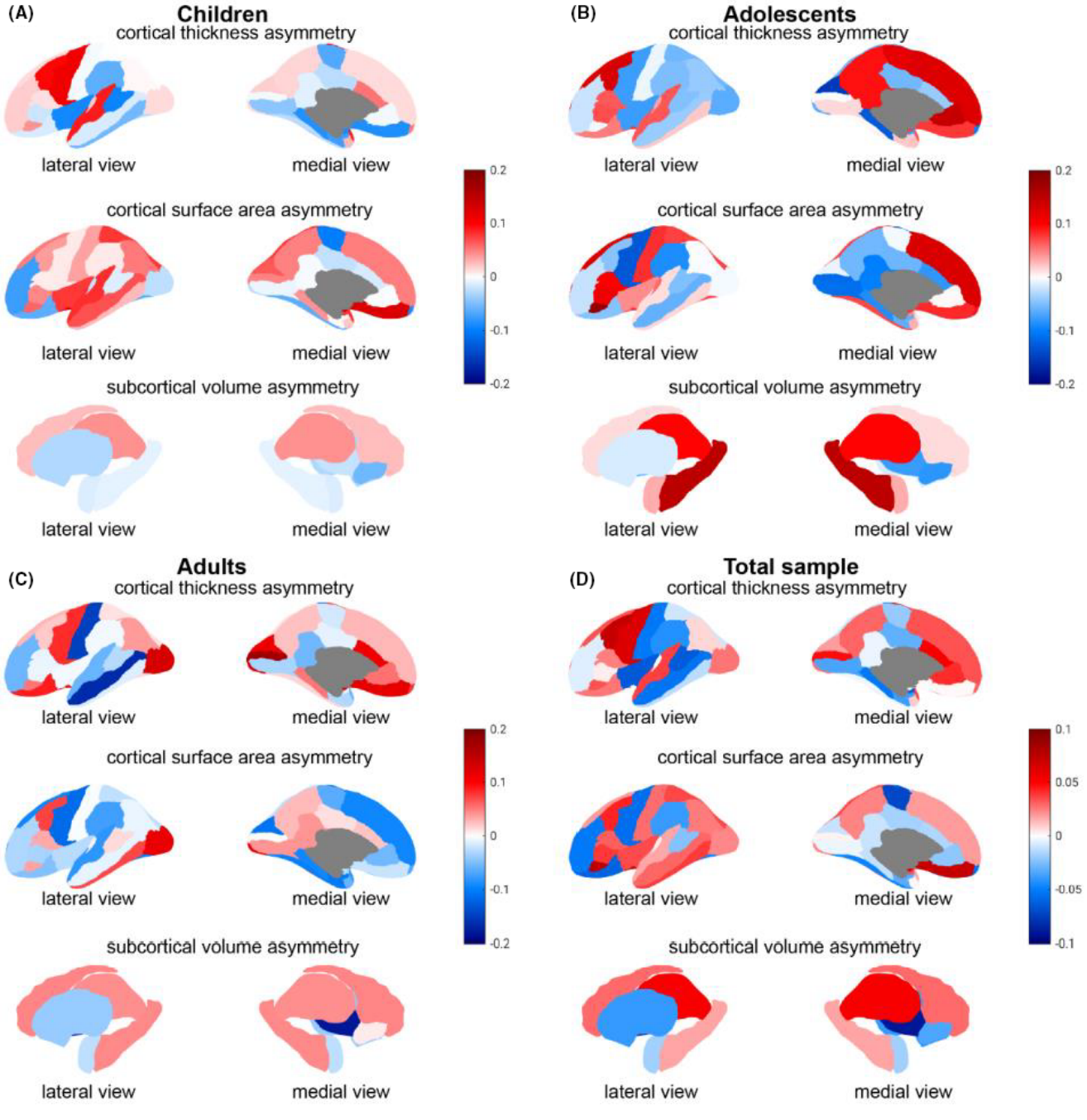

Figure 1 Cohen's *d* effect sizes of the associations between ADHD diagnosis and AIs of subcortical volumes, cortical surface areas and cortical thicknesses for (A) children, (B) adolescents, (C) adults, and (D) all age groups combined. Positive values *(red)* indicate mean shifts towards greater leftward or reduced rightward asymmetry in ADHD, and negative values (*blue*) indicate mean shifts towards greater rightward asymmetry or reduced leftward asymmetry in ADHD.

differences between datasets, although between-dataset heterogeneity that affected model coefficients within datasets would not be fully accounted by this approach. While the random-intercept model cannot fully rescue power in the case that effects are truly specific to certain subsets, no single center has been able to collect such a large ADHD-control sample alone. Our large sample size yields accurate estimates of effect sizes with respect to the overall case–control population, as represented across many research centers. In this way, the findings from multi-center studies such as ours can be considered more generalizable than single-center studies (Costafreda, 2009). In any case, as long as researchers publish separate papers based on many single, smaller datasets, collected in particular ways, the field overall has the same issue of heterogeneity. Of note, the ENIGMA consortium previously showed that using the random-intercept approach to account for dataset heterogeneity is similar to random effect meta-analysis across datasets, but preferable because it produces lower standard errors and

narrower confidence intervals than meta-analysis (Boedhoe et al., 2018).

Although not a longitudinal study, our data spanned a wide age range from childhood through to older adulthood, which allowed us to study different age groups separately, as the disorder may be neurobiologically distinct in different age groups (Alexander & Farrelly, 2018; Hoogman et al., 2019). The previous ENIGMA study of bilateral cortical differences in ADHD found children to be most affected, particularly in frontal, cingulate, and temporal regions, as well as the total hemispheric surface area, which was lower in ADHD (Hoogman et al., 2019). In the children-only analysis in our present study of asymmetries, we also found associations with diagnosis for some frontal and temporal regions (including the caudal middle frontal cortex thickness, precentral gyrus thickness, medial orbitofrontal cortex surface area, banks of the superior temporal sulcus thickness), as well as a change in the asymmetry of total hemispheric surface area, driven by a greater decrease of area in ADHD on the right-side than the left-side. These findings offer a more nuanced description of brain changes in childhood ADHD, which may involve altered lateralized neurodevelopment.

However, considering all brain asymmetry measures, the effect sizes in the present study were not stronger in children as compared to adolescents or adults. Furthermore, bilateral case–control differences are not necessarily a good guide to case–control differences in asymmetry, since a difference in asymmetry can arise, for example, from a simultaneous left-sided increase and right-sided decrease in a brain measure, which can involve no change at all in the bilateral measure. Hence, we took a screening approach to the present study, rather than constraining our search on prior bilateral findings. It is also not entirely clear how/whether to statistically adjust the test for total hemispheric surface asymmetry, in the context of also testing multiple subregions, and also with respect to study-wide multiple testing. Therefore, we present all *p*-values unadjusted, while also being mindful of the tentative nature of these findings in the context of our survey across many brain asymmetry measures. Together with the corresponding effect size estimates, this mapping information should be useful for the field.

We did not include handedness, IQ, or brain size as covariates in our primary analysis, in order to avoid possible collider bias (Cole et al., 2010), as there are various plausible causal relations linking these traits with ADHD, brain asymmetry and other, possibly underlying factors shared between some or all of them. For example, having the disorder for other underlying reasons may lead to altered asymmetry and brain size, or altered asymmetry and brain size may contribute to having the disorder. A priori, altered asymmetry may not be associated with the disorder, but be associated with brain size, which can be associated with disorder. In this latter case, correcting for brain size can induce spurious associations between asymmetry and disorder. Collider bias is under-appreciated in the field, perhaps because it is not intuitive. Alternatively, including brain size as a covariate in case–control analysis might have reduced the power to detect an association of diagnosis with asymmetry. This would occur if underlying susceptibility factors contribute both to altered asymmetry and reduced brain size, as part of the ADHD phenotype. Regardless, our primary interest was to detect associations of diagnosis with asymmetry regardless of other brain features such as overall size. We have made available, in supplementary csv files, the results from secondary analyses in which we included handedness, IQ, or intracranial volume as covariates, with or without interaction terms with case–control status. As regards handedness specifically, previous studies of subcortical and cortical anatomical asymmetry in over 15,000 subjects from healthy control and population datasets, also performed by the ENIGMA consortium (Guadalupe et al., 2016; Kong et al., 2018), found no significant effects of handedness.

Our study was limited to macro-anatomical asymmetries of cortical gray matter and subcortical volumes. It is possible that altered brain asymmetry in ADHD will be more apparent in different structural or functional modalities, or at different scales. For example, cortical thickness measures can correlate with the degree of myelination (Natu et al., 2019), such that quantitative neuroimaging methods that are sensitive to microstructural tissue content may reveal further alterations in ADHD. At a larger scale, asymmetries of white matter tracts (Wu et al., 2020) may also benefit from the large-scale approach that we have used here. Asymmetries of functional asymmetry, particularly linked to attentional tasks, may also reveal stronger case–control differences than the structural effects we observed (see Introduction).

Conclusion

We carried out the largest case–control study of structural brain asymmetry in ADHD. We described average changes of asymmetry that are small, but helpful towards a more complete description of brain anatomical changes in this disorder. Results were largely discrepant with earlier, inconsistent findings from smaller-scale studies, which illustrates the value of taking a large-scale approach to human clinical neuroscience. The small effects that we found remain statistically tentative in the context of multiple testing, even in this unprecedented sample size. Future longitudinal and genetic studies may probe causative relations between ADHD and brain asymmetry, focused on measures defined from this study, such as total hemispheric surface area asymmetry, medial orbitofrontal area asymmetry, or globus pallidus volume asymmetry.

Supporting information

Additional supporting information may be found online in the Supporting Information section at the end of the article:

Supplementary Methods

Table S1. Characteristics of the different datasets.

Table S2. Full linear model results for the subcortical volume AIs in children.

Table S3. Full linear model results for the cortical surface area AIs in children.

Table S4. Full linear model results for the cortical thickness AIs in children.

Table S5. Full linear model results for the subcortical volume AIs in adolescents.

Table S6. Full linear model results for the cortical surface area AIs in adolescents.

Table S7. Full linear model results for the cortical thickness AIs in adolescents.

Table S8. Full linear model results for the subcortical volume AIs in adults.

Table S9. Full linear model results for the cortical surface area AIs in adults.

Table S10. Full linear model results for the cortical thickness AIs in adults.

Table S11. Full linear model results for the subcortical volume AIs in all age groups combined.

Table S12. Full linear model results for the cortical surface area AI in all age groups combined.

Table S13. Full linear model results for the cortical thickness AIs in all age groups combined.

Table S14. Directions of asymmetry changes in ADHD individuals versus controls for those AIs that had shown nominally significant ($p < .05$) associations with diagnosis in any of the main analyses.

Table S15. Sensitivity analyses for the effects of diagnosis in all age groups combined, for subcortical volume AIs.

Table S16. Sensitivity analyses for the effects of diagnosis in all age groups combined, for cortical surface area AIs.

Table S17. Sensitivity analyses for the effects of diagnosis in all age groups combined, for cortical thickness AIs.

Table S18. Associations of subcortical volume AIs with disorder severity in ADHD individuals, all age groups combined.

Table S19. Associations of cortical surface area AIs with disorder severity in ADHD individuals, all age groups combined.

Table S20. Associations of cortical thickness AIs with disorder severity in ADHD individuals, all age groups combined.

Table S21. Associations of subcortical volume AIs with psychostimulant medication use in ADHD individuals, all age groups combined.

Table S22. Associations of cortical surface area AIs with psychostimulant medication use in ADHD individuals, all age groups combined.

Table S23. Associations of cortical thickness AIs with psychostimulant medication use in ADHD individuals, all age groups combined.

Table S24. Associations of subcortical volume AIs with comorbidities in ADHD individuals, all age groups combined.

Table S25. Associations of cortical surface area AIs with comorbidities in ADHD individuals, all age groups combined.

Table S26. Associations of cortical thickness AIs with comorbidities in ADHD individuals, all age groups combined.

Table S27. Associations of subcortical volume AIs with IQ in all age groups combined.

Table S28. Associations of cortical surface area AIs with IQ in all age groups combined.

Table S29. Associations of cortical thickness AIs with IQ in all age groups combined.

Figure S1. Joyplot of the distributions of AIs in the total study sample (without winsorization), in ADHD cases and controls.

Figure S2. Correlations between AIs of subcortical volumes in the total study sample, as well as in cases and controls.

Figure S3. Correlations between AIs of cortical surface areas in the total study sample, cases, and controls.

Figure S4. Correlations between AIs of cortical thickness in the total study sample, cases, and controls.

Figure S5. Residual plots of the linear mixed effects model analysis of subcortical volume AIs in the total study sample.

Figure S6. Residual plots of the linear mixed effects model analysis of cortical surface area AIs and the AI of the total average surface area (totalsurf) in the total study sample.

Figure S7. Residual plots of the linear mixed effects model analysis of cortical thickness AIs and the AI of the total average thickness (totalthick) in the total study sample.

Figure S8. Scatter plots of the relationship between age and AIs of the subcortical volumes.

Figure S9. Scatter plots of the relationship between age and AIs of the cortical surface areas.

Figure S10. Scatter plots of the relationship between age and AIs of the cortical thickness.

Figure S11. Distributions of age, sex, handedness, IQ and ICV in ADHD and controls.

Figure S12. Distributions within ADHD cases of hyperactivity/impulsivity symptom scores, inattention symptom scores, medication status, and comorbidity status.

Figure S13. Bar plots of the Cohen's *d* effect sizes for diagnosis in the different age groups analyzed.

Supplementary References

Acknowledgments

Mr. Earl is co-inventor of the Oregon Health and Science University Technology #2198 (co-owned with Washington University in St. Louis), FIRMM: Real time monitoring and prediction of motion in MRI scans, exclusively licensed to Nous, Inc.) and any related research. Any potential conflict of interest has been reviewed and managed by OHSU. Dr. Biederman has received research support from AACAP, Alcobra, the Feinstein Institute for Medical Research, the Forest Research Institute,

Genentech, Headspace, Ironshore, Lundbeck AS, Magceutics, Merck, Neurocentria, NIDA, NIH, PamLab, Pfizer, Roche TCRC, Shire, SPRITES, Sunovion, the U.S. Department of Defense, the U.S. Food and Drug Administration, and Vaya Pharma/Enzymotec; he has served as a consultant or on scientific advisory boards for Aevi Genomics, Akili, Alcobra, Arbor Pharmaceuticals, Guidepoint, Ironshore, Jazz Pharma, Medgenics, Piper Jaffray, and Shire; he has received honoraria from Alcobra, the American Professional Society of ADHD and Related Disorders, and the MGH Psychiatry Academy for tuition-funded CME courses; he has a financial interest in Avekshan, a company that develops treatments for ADHD; he has a U.S. patent application pending (Provisional Number #61/233,686) through MGH corporate licensing, on a method to prevent stimulant abuse; and his program has received royalties from a copyrighted rating scale used for ADHD diagnoses, paid to the Department of Psychiatry at Massachusetts General Hospital by Ingenix, Prophase, Shire, Bracket Global, Sunovion, and Theravance. Dr. Van Erp has served as consultant for Roche Pharmaceuticals and has a contract with Otsuka Pharmaceutical, Ltd. Dr. Gabel has received funding from the Motor Neurone Disease Association. Dr. Asherson has served as a consultant and as a speaker at sponsored events for Eli Lilly, Novartis, and Shire, and he has received educational/research awards from Eli Lilly, GW Pharma, Novartis, QbTech, Shire, and Vifor Pharma. Dr. Brandeis has served as an unpaid scientific consultant for an EU-funded neurofeedback trial. Dr. Karkashadze has received payment for article authorship and speaking fees from Sanofi and from Pikfarma. Dr. Mattos has served on speakers' bureau and/or as a consultant for Janssen-Cilag, Novartis, and Shire and has received travel awards from those companies to participate in scientific meetings; the ADHD outpatient program (Grupo de Estudos do Déficit de Atenção/Institute of Psychiatry) chaired by Dr. Mattos also received research support from Novartis and Shire. Dr. Banaschewski served in an advisory or consultancy role for Lundbeck, Medice, Neurim Pharmaceuticals, Oberberg GmbH, Shire, and Infectopharm. He received conference support or speaker's fee from Lilly, Medice, and Shire. He received royalties from Hogrefe, Kohlhammer, CIP Medien, Oxford University Press; the present work is unrelated to these relationships. Dr. Paloyelis has received an unrestricted research grant from PARI GmbH. Dr. Coghill has served in an advisory or consultancy role for Eli Lilly, Medice, Novartis, Oxford Outcomes, Shire, and Vifor Pharma; he has received conference support or speaking fees from Eli Lilly, Janssen McNeil, Medice, Novartis, Shire, and Sunovion; and he has been involved in clinical trials conducted by Eli Lilly and Shire. Dr. Kuntsi has received speaking honoraria and advisory panel payments for participation at educational events sponsored by Medice; all funds are received by King's College London and used for studies of ADHD. Dr. Mehta has received research funding from Lundbeck, Shire, and Takeda and has served on advisory boards for Lundbeck and Autifony. Dr. Harrison has received research funding from Janssen Pharmaceuticals. Dr. Bellgrove has received speaking fees and travel support from Shire. Dr. Rubia has received a grants from Eli Lilly/Takeda pharmaceuticals for another project. Dr. Walitza has received lecture honoraria from Eli Lilly and OpoPharma, support from the Hartmann Müller, Olga Mayenfisch, and Gertrud Thalmann foundations, and royalties from Beltz, Hogrefe, Kohlhammer, Springer, and Thieme. Dr. Haavik has received speaking fees from Biocodex, Eli Lilly, HB Pharma, Janssen-Cilag, Medice, Novartis, and Shire. Dr. Lesch has served as a speaker for Eli Lilly and has received research support from Medice and travel support from Shire. Dr. Reif has received honoraria for serving as speaking or on advisory boards for Janssen, Medice, Neuraxpharm, Servier and Shire. Dr. Konrad has received speaking fees from Eli Lilly, Medice, and Shire. Dr. Hoekstra served on the advisory board for Shire. Dr. Ramos-Quiroga has served on the speakers bureaus and/or as a consultant for Almirall, Braingaze, Eli Lilly, Janssen-Cilag, Lundbeck, Medice, Novartis, Shire, Takeda, Shionogui, Bial, Sincrolab, and Rubió; he has received travel awards for taking part in psychiatric meetings from Eli Lilly, Janssen-Cilag, Medice, Rubió, and Shire, Takeda, Bial, Shionogui; and the Department of Psychiatry chaired by him has received unrestricted educational and research support from Actelion, Eli Lilly, Ferrer, Janssen-Cilag, Lundbeck, Oryzon, Psious, Roche, Rubió, and Shire. Dr. Fair is a founder of Nous Imaging, Inc.; any potential conflicts of interest are being reviewed and managed by OHSU. Dr. Thompson has received funding support from Biogen. Dr. Buitelaar has served as a consultant, advisory board member, and/or speaker for Eli Lilly, JanssenCilag, Medice, Roche, Takeda/Shire, Angelini, and Servier. Dr. Faraone has received income, potential income, travel expenses, continuing education support, and/or research support from Akili Interactive Labs, Alcobra, Arbor, Enzymotec, Genomind, Ironshore, Janssen, KemPharm, McNeil, Neurolifesciences, NeuroVance, Novartis, Otsuka, Pfizer, Rhodes, Shire/Takeda, Sunovion, Supernus, Tris, and Medice; he receives royalties from Elsevier, Guilford Press, and Oxford University Press; he is principal investigator of www.adhdinadults.com; and, with his institution, he holds U.S. patent US20130217707 A1 for the use of sodium-hydrogen exchange inhibitors in the treatment of ADHD. Dr. Franke has received educational speaking fees from Shire and Medice**.** All remaining authors reported no biomedical financial interests or potential conflicts of interests. Open Access funding enabled and organized by Projekt DEAL.

Correspondence

Clyde Francks, Max Planck Institute for Psycholinguistics, Wundtlaan 1, Nijmegen, The Netherlands; Email: clyde.francks@mpi.nl

Key points

- The extent to which brain anatomical asymmetry is altered in ADHD has remained unclear. Previous studies of brain asymmetry in ADHD were based on small sample sizes, so that findings may have been unreliable.
- We carried out the largest-ever study of brain anatomical asymmetry in ADHD. Average case-control differences of asymmetry were very small, and the regions implicated were largely discrepant with earlier findings based on smaller samples.
- This study illustrates the value of a large-scale approach to human clinical neuroscience. The findings provide an improved description of brain anatomical changes in ADHD.
- Of itself, altered anatomical asymmetry is not likely to be a useful biomarker for ADHD. Future longitudinal and genetic studies may probe causative relations between ADHD and asymmetry of the total hemispheric surface area, medial orbitofrontal area, and globus pallidus volume.

References

Alexander, L., & Farrelly, N. (2018). Attending to adult ADHD: A review of the neurobiology behind adult ADHD. *Irish Journal of Psychological Medicine*, *35*, 237–244.

American Psychiatric Association. (2000). *Diagnostic and statistical manual of mental disorders*. 4th (DSM-IV), ed. Washington DC: American Psychiatric Association.

American Psychiatric Association (2013). *Diagnostic and statistical manual of mental disorders*, 5th ed. Washington, DC: American Psychiatric Association.

Baribeau, D.A., Dupuis, A., Paton, T.A., Hammill, C., Scherer, S.W., Schachar, R.J., … & Anagnostou, E. (2019). Structural neuroimaging correlates of social deficits are similar in autism spectrum disorder and attention-deficit/hyperactivity disorder: Analysis from the POND Network. *Transl Psychiatry*, *9*, 72.

Benjamini, Y., & Hochberg, Y. (1995). Controlling the false discovery rate - A practical and powerful approach to multiple testing. *Journal of the Royal Statistical Society Series B-Methodological*, *57*, 289–300.

Biberacher, V., Schmidt, P., Keshavan, A., Boucard, C.C., Righart, R., Sämann, P., … & Mühlau, M. (2016). Intra- and interscanner variability of magnetic resonance imaging based volumetry in multiple sclerosis. *NeuroImage*, *142*, 188–197.

Bishop, D.V. (2013). Cerebral asymmetry and language development: cause, correlate, or consequence? *Science*, *340*, 1230531.

Boedhoe, P.S.W., Heymans, M.W., Schmaal, L., Abe, Y., Alonso, P., Ameis, S.H., … & Twisk, J.W.R. (2018). An empirical comparison of meta- and mega-analysis with data from the ENIGMA Obsessive-Compulsive Disorder Working Group. *Front Neuroinform*, *12*, 102.

Boedhoe, P.S.W., van Rooij, D., Hoogman, M., Twisk, J.W.R., Schmaal, L., Abe, Y. … & Calderoni, S. (2019). Subcortical brain volume, regional cortical thickness and cortical surface area across attention-deficit/hyperactivity disorder (ADHD), autism spectrum disorder (ASD), and obsessive-compulsive disorder (OCD). bioRxiv. https://doi.org/10.1101/673012

Button, K.S., Ioannidis, J.P., Mokrysz, C., Nosek, B.A., Flint, J., Robinson, E.S., & Munafo, M.R. (2013). Power failure: Why small sample size undermines the reliability of neuroscience. *Nature Reviews Neuroscience*, *14*, 365–376.

Cao, Q., Wang, J., Sun, L., Wang, P., Wu, Z., & Wang, Y. (2014). Altered anatomical asymmetry in children with attention deficit/hyperactivity disorder: A pilot optimized voxel-based morphometric study. *Zhonghua Yi Xue Za Zhi*, *94*, 3387–3391.

Castellanos, F.X., Giedd, J.N., Marsh, W.L., Hamburger, S.D., Vaituzis, A.C., Dickstein, D.P., … & Rapoport, J.L. (1996). Quantitative brain magnetic resonance imaging in attention-deficit hyperactivity disorder. *Archives of General Psychiatry*, *53*, 607–616.

Chambers, J.M., & Hastie, T.J. (1992). *Statistical models in S*. Pacific Grove, CA: Wadsworth & Brooks/Cole.

Chung, J., Yoo, K., Lee, P., Kim, C.M., Roh, J.H., Park, J.E., … & Jeong, Y. (2017). Normalization of cortical thickness measurements across different T1 magnetic resonance imaging protocols by novel W-Score standardization. *NeuroImage*, *159*, 224–235.

Cole, S.R., Platt, R.W., Schisterman, E.F., Chu, H., Westreich, D., Richardson, D., & Poole, C. (2010). Illustrating bias due to conditioning on a collider. *International Journal of Epidemiology*, *39*, 417–420.

Cortese, S., Kelly, C., Chabernaud, C., Proal, E., Di Martino, A., Milham, M.P., & Castellanos, F.X. (2012). Toward systems neuroscience of ADHD: A meta-analysis of 55 fMRI studies. *American Journal of Psychiatry*, *169*, 1038–1055.

Costafreda, S. (2009). Pooling fMRI data: Meta-analysis, mega-analysis and multi-center studies. *Frontiers Neuroinformatics*, *3*(33), https://doi.org/10.3389/neuro.11.033.2009

Dang, L.C., Samanez-Larkin, G.R., Young, J.S., Cowan, R.L., Kessler, R.M., & Zald, D.H. (2016). Caudate asymmetry is related to attentional impulsivity and an objective measure of ADHD-like attentional problems in healthy adults. *Brain Structure and Function*, *221*, 277–286.

Demopoulos, C., Hopkins, J., & Davis, A. (2013). A comparison of social cognitive profiles in children with autism spectrum disorders and attention-deficit/hyperactivity disorder: A matter of quantitative but not qualitative difference? *Journal of Autism and Developmental Disorders*, *43*, 1157–1170.

Desikan, R.S., Ségonne, F., Fischl, B., Quinn, B.T., Dickerson, B.C., Blacker, D., … & Killiany, R.J. (2006). An automated labeling system for subdividing the human cerebral cortex on MRI scans into gyral based regions of interest. *NeuroImage*, *31*, 968–980.

Douglas, P.K., Gutman, B., Anderson, A., Larios, C., Lawrence, K.E., Narr, K., … & Bookheimer, S.Y. (2018). Hemispheric brain asymmetry differences in youths with attention-deficit/hyperactivity disorder. *NeuroImage Clinical*, *18*, 744–752.

Duboc, V., Dufourcq, P., Blader, P., & Roussigne, M. (2015). Asymmetry of the brain: Development and implications. *Annual Review of Genetics*, *49*, 647–672.

Ellison-Wright, I., Ellison-Wright, Z., & Bullmore, E. (2008). Structural brain change in Attention Deficit Hyperactivity Disorder identified by meta-analysis. *BMC Psychiatry*, *8*, 51.

Faraone, S.V., Asherson, P., Banaschewski, T., Biederman, J., Buitelaar, J.K., Ramos-Quiroga, J.A., … & Franke, B. (2015). Attention-deficit/hyperactivity disorder. *Nature Reviews Disease Primers*, *1*, 15020.

Fayyad, J., Sampson, N.A., Hwang, I., Adamowski, T., Aguilar-Gaxiola, S., Al-Hamzawi, A., … & Kessler, R.C. (2017). The descriptive epidemiology of DSM-IV Adult ADHD in the

World Health Organization World Mental Health Surveys. *Attention Deficit and Hyperactivity Disorders*, *9*, 47–65.
Filipek, P.A., SemrudClikeman, M., Steingard, R.J., Renshaw, P.F., Kennedy, D.N., & Biederman, J. (1997). Volumetric MRI analysis comparing subjects having attention-deficit hyperactivity disorder with normal controls. *Neurology*, *48*, 589–601.
Fischl, B. (2012). FreeSurfer. *NeuroImage*, *62*, 774–781.
Fortin, J.-P., Cullen, N., Sheline, Y.I., Taylor, W.D., Aselcioglu, I., Cook, P.A., … & Shinohara, R.T. (2018). Harmonization of cortical thickness measurements across scanners and sites. *NeuroImage*, *167*, 104–120.
Geeraerts, S., Lafosse, C., Vaes, N., Vandenbussche, E., & Verfaillie, K. (2008). Dysfunction of right-hemisphere attentional networks in attention deficit hyperactivity disorder. *Journal of Clinical and Experimental Neuropsychology*, *30*, 42–52.
Ghirardi, L., Pettersson, E., Taylor, M.J., Freitag, C.M., Franke, B., Asherson, P., … & Kuja-Halkola, R. (2019). Genetic and environmental contribution to the overlap between ADHD and ASD trait dimensions in young adults: A twin study. *Psychological Medicine*, *49*, 1713–1721.
Guadalupe, T., Mathias, S.R., vanErp, T.G.M., Whelan, C.D., Zwiers, M.P., Abe, Y., … & Francks, C. (2016). Human subcortical brain asymmetries in 15,847 people worldwide reveal effects of age and sex. *Brain Imaging and Behavior*, *11*, 1497–1514.
Guadalupe, T., Zwiers, M.P., Teumer, A., Wittfeld, K., Vasquez, A.A., Hoogman, M., … & Francks, C. (2014). Measurement and genetics of human subcortical and hippocampal asymmetries in large datasets. *Human Brain Mapping*, *35*, 3277–3289.
Hale, T.S., Kane, A.M., Kaminsky, O., Tung, K.L., Wiley, J.F., McGough, J.J., … & Kaplan, J.T. (2014). Visual network asymmetry and default mode network function in ADHD: An fMRI study. *Frontiers in Psychiatry*, *5*, 81.
Hale, T.S., Loo, S.K., Zaidel, E., Hanada, G., Macion, J., & Smalley, S.L. (2009). Rethinking a right hemisphere deficit in ADHD. *Journal of Attention Disorders*, *13*, 3–17.
Hale, T.S., Smalley, S.L., Walshaw, P.D., Hanada, G., Macion, J., McCracken, J.T., … & Loo, S.K. (2010). Atypical EEG beta asymmetry in adults with ADHD. *Neuropsychologia*, *48*, 3532–3539.
Heilman, K.M., Bowers, D., Valenstein, E., & Watson, R.T. (1986). The right hemisphere: Neuropsychological functions. *Journal of Neurosurgery*, *64*, 693–704.
Hoogman, M., Bralten, J., Hibar, D.P., Mennes, M., Zwiers, M.P., Schweren, L.S.J., … & Franke, B. (2017). Subcortical brain volume differences in participants with attention deficit hyperactivity disorder in children and adults: A cross-sectional mega-analysis. *Lancet Psychiatry*, *4*, 310–319.
Hoogman, M., Muetzel, R., Guimaraes, J.P., Shumskaya, E., Mennes, M., Zwiers, M.P., … & Franke, B. (2019). Brain imaging of the cortex in ADHD: A coordinated analysis of large-scale clinical and population-based samples. *American Journal of Psychiatry*, *176*, 531–542.
Hynd, G.W., Hern, K.L., Novey, E.S., Eliopulos, D., Marshall, R., Gonzalez, J.J., & Voeller, K.K. (1993). Attention deficit-hyperactivity disorder and asymmetry of the caudate nucleus. *Journal of Child Neurology*, *8*, 339–347.
Kang, X., Herron, T.J., Cate, A.D., Yund, E.W., & Woods, D.L. (2012). Hemispherically-unified surface maps of human cerebral cortex: Reliability and hemispheric asymmetries. *PLoS One*, *7*, e45582.
Kong, X.-Z., Mathias, S.R., Guadalupe, T., Glahn, D.C., Franke, B., Crivello, F., … & Francks, C. (2018). Mapping cortical brain asymmetry in 17,141 healthy individuals worldwide via the ENIGMA Consortium. *Proceedings of the National Academy of Sciences*, *115*, E5154–E5163.
Kurth, F., Gaser, C., & Luders, E. (2015). A 12-step user guide for analyzing voxel-wise gray matter asymmetries in statistical parametric mapping (SPM). *Nature Protocols*, *10*, 293–304.
Langleben, D.D., Austin, G., Krikorian, G., Ridlehuber, H.W., Goris, M.L., & Strauss, H.W. (2001). Interhemispheric asymmetry of regional cerebral blood flow in prepubescent boys with attention deficit hyperactivity disorder. *Nuclear Medicine Communications*, *22*, 1333–1340.
Leitner, Y. (2014). The co-occurrence of autism and attention deficit hyperactivity disorder in children - what do we know? *Frontiers in Human Neuroscience*, *8*, 268.
Leroy, F., Cai, Q., Bogart, S.L., Dubois, J., Coulon, O., Monzalvo, K., … & Dehaene-Lambertz, G. (2015). New human-specific brain landmark: The depth asymmetry of superior temporal sulcus. *Proceedings of the National Academy of Sciences*, *112*, 1208–1213.
Li, D., Li, T., Niu, Y., Xiang, J., Cao, R., Liu, B.O., … & Wang, B. (2018). Reduced hemispheric asymmetry of brain anatomical networks in attention deficit hyperactivity disorder. *Brain Imaging Behav*, *13*, 669–684.
Li, X., Jiang, J., Zhu, W., Yu, C., Sui, M., Wang, Y., & Jiang, T. (2007). Asymmetry of prefrontal cortical convolution complexity in males with attention-deficit/hyperactivity disorder using fractal information dimension. *Brain and Development*, *29*, 649–655.
Maingault, S., Tzourio-Mazoyer, N., Mazoyer, B., & Crivello, F. (2016). Regional correlations between cortical thickness and surface area asymmetries: A surface-based morphometry study of 250 adults. *Neuropsychologia*, *93*(Pt B), 350–364.
Mohamed, S.M., Börger, N.A., Geuze, R.H., & van der Meere, J.J. (2016). Linking state regulation, brain laterality, and self-reported attention-deficit/hyperactivity disorder (ADHD) symptoms in adults. *Journal of Clinical and Experimental Neuropsychology*, *38*, 831–843.
Munafo, M.R., & Flint, J. (2010). How reliable are scientific studies? *British Journal of Psychiatry*, *197*, 257–258.
Münte, T.F., Marco-Pallares, J., Bolat, S., Heldmann, M., Lütjens, G., Nager, W., … & Krauss, J.K. (2017). The human globus pallidus internus is sensitive to rewards – Evidence from intracerebral recordings. *Brain Stimulation*, *10*, 657–663.
Nakao, T., Radua, J., Rubia, K., & Mataix-Cols, D. (2011). Gray matter volume abnormalities in ADHD: Voxel-based meta-analysis exploring the effects of age and stimulant medication. *American Journal of Psychiatry*, *168*, 1154–1163.
Natu, V.S., Gomez, J., Barnett, M., Jeska, B., Kirilina, E., Jaeger, C., … & Grill-Spector, K. (2019). Apparent thinning of human visual cortex during childhood is associated with myelination. *Proceedings of the National Academy of Sciences*, *116*, 20750–20759.
Panizzon, M.S., Fennema-Notestine, C., Eyler, L.T., Jernigan, T.L., Prom-Wormley, E., Neale, M., … & Kremen, W.S. (2009). Distinct genetic influences on cortical surface area and cortical thickness. *Cerebral Cortex*, *19*, 2728–2735.
Pardoe, H.R., Pell, G.S., Abbott, D.F., & Jackson, G.D. (2009). Hippocampal volume assessment in temporal lobe epilepsy: How good is automated segmentation? *Epilepsia*, *50*, 2586–2592.
Perlaki, G., Horvath, R., Nagy, S.A., Bogner, P., Doczi, T., Janszky, J., & Orsi, G. (2017). Comparison of accuracy between FSL's FIRST and Freesurfer for caudate nucleus and putamen segmentation. *Scientific Reports*, *7*, 2418.
Polanczyk, G., de Lima, M.S., Horta, B.L., Biederman, J., & Rohde, L.A. (2007). The worldwide prevalence of ADHD: a systematic review and metaregression analysis. *American Journal of Psychiatry*, *164*, 942–948.
Postema, M.C., van Rooij, D., Anagnostou, E., Arango, C., Auzias, G., Behrmann, M., … & Francks, C. (2019). Altered structural brain asymmetry in autism spectrum disorder in a study of 54 datasets. *Nature Communications*, *10*, 4958.
Pretus, C., Ramos-Quiroga, J.A., Richarte, V., Corrales, M., Picado, M., Carmona, S., & Vilarroya, O. (2017). Time and

psychostimulants: Opposing long-term structural effects in the adult ADHD brain. A longitudinal MR study. *European Neuropsychopharmacology*, *27*, 1238–1247.

Radonjić, N.V., Hess, J.L., Rovira, P., Andreassen, O., Buitelaar, J.K., Ching, C.R.K. … & Faraone, S.V. (2019). Structural brain imaging studies offer clues about the effects of the shared genetic etiology among neuropsychiatric disorders. bioRxiv.

Reale, L., Bartoli, B., Cartabia, M., Zanetti, M., Costantino, M.A., Canevini, M.P., … & Bonati, M. (2017). Comorbidity prevalence and treatment outcome in children and adolescents with ADHD. *European Child and Adolescent Psychiatry*, *26*, 1443–1457.

Renteria, M.E. (2012). Cerebral asymmetry: A quantitative, multifactorial, and plastic brain phenotype. *Twin Research and Human Genetics*, *15*, 401–413.

Schrimsher, G.W., Billingsley, R.L., Jackson, E.F., & Moore, B.D., 3rd (2002). Caudate nucleus volume asymmetry predicts attention-deficit hyperactivity disorder (ADHD) symptomatology in children. *Journal of Child Neurology*, *17*, 877–884.

Shaw, P., Lalonde, F., Lepage, C., Rabin, C., Eckstrand, K., Sharp, W., … & Rapoport, J. (2009). Development of cortical asymmetry in typically developing children and its disruption in attention-deficit/hyperactivity disorder. *Archives of General Psychiatry*, *66*, 888–896.

Stefanatos, G.A., & Wasserstein, J. (2001). Attention deficit/hyperactivity disorder as a right hemisphere syndrome. Selective literature review and detailed neuropsychological case studies. *Annals of the New York Academy of Sciences*, *931*, 172–195.

Stergiakouli, E., Davey Smith, G., Martin, J., Skuse, D.H., Viechtbauer, W., Ring, S.M., … & St Pourcain, B. (2017). Shared genetic influences between dimensional ASD and ADHD symptoms during child and adolescent development. *Molecular Autism*, *8*, 18.

Toga, A.W., & Thompson, P.M. (2003). Mapping brain asymmetry. *Nature Reviews Neuroscience*, *4*, 37–48.

Uhlikova, P., Paclt, I., Vaneckova, M., Morcinek, T., Seidel, Z., Krasensky, J., & Danes, J. (2007). Asymmetry of basal ganglia in children with attention deficit hyperactivity disorder. *Neuro Endocrinol Lett*, *28*, 604–609.

van der Meer, J.M., Oerlemans, A.M., van Steijn, D.J., Lappenschaar, M.G., de Sonneville, L.M., Buitelaar, J.K., & Rommelse, N.N. (2012). Are autism spectrum disorder and attention-deficit/hyperactivity disorder different manifestations of one overarching disorder? Cognitive and symptom evidence from a clinical and population-based sample. *Journal of the American Academy of Child and Adolescent Psychiatry*, *51*, 1160–1172.e1163.

Vance, A., Silk, T.J., Casey, M., Rinehart, N.J., Bradshaw, J.L., Bellgrove, M.A., & Cunnington, R. (2007). Right parietal dysfunction in children with attention deficit hyperactivity disorder, combined type: A functional MRI study. *Molecular Psychiatry*, *12*(9), 826–832.

World Health Organization (1992). *International classification of diseases and related health problems, 10th revision*. Geneva: World Health Organization.

Wu, Z.-M., Wang, P., Yang, L.I., Liu, L.U., Sun, L.I., An, L.I., … & Wang, Y.-F. (2020). Altered brain white matter microstructural asymmetry in children with ADHD. *Psychiatry Research*, *285*, 112817.

Yaakub, S.N., Heckemann, R.A., Keller, S.S., McGinnity, C.J., Weber, B., & Hammers, A. (2020). On brain atlas choice and automatic segmentation methods: A comparison of MAPER & FreeSurfer using three atlas databases. *Scientific Reports*, *10*, 2837.

Zou, H., & Yang, J. (2019). Temporal variability-based functional brain lateralization study in ADHD. *Journal of Attention Disorders*, 1087054719859074. https://doi.org/10.1177/1087054719859074

Accepted for publication: 19 December 2020